UNIVERSITY OF CALIFORNIA SAN DIEGO

Modeling MeCP2 loss-of-function in human iPSC-derived astrocytes highlights LINE-1 retrotransposon as contributor to neuroinflammation

A Thesis submitted in partial satisfaction of the requirements for the degree
Master of Science

in

Biology

by

Aurian Saleh

Committee in Charge:

Professor Alysson Muotri, Chair
Professor Douglass Forbes, Co-Chair
Professor Stacey Glasgow

2020

The Thesis of Aurian Saleh is approved, and it is acceptable in quality and form for publication on microfilm and electronically:

_____

_____
Co-Chair

_____
Chair

University of California San Diego

2020

DEDICATION

I dedicate this thesis to my mom, Hasina. Thank you for your unwavering love and support.

TABLE OF CONTENTS

LIST OF ABBREVIATIONS

3D: 3-dimensional

3TC: lamivudine, a nucleoside analog reverse-transcriptase inhibitor

ASD: autism spectrum disorder

BDNF: brain-derived neurotrophic factor

ChIP: chromatin immunoprecipitation

CpG: cytosine nucleotide followed by guanine nucleotide going from 5' to 3'

CREB: cAMP response element binding protein

CTRL: control

CNTF: ciliary neurotrophic factor

d4T: stavudine, a nucleoside analog reverse-transcriptase inhibitor

DMSO: dimethyl sulfoxide

DNA: deoxyribonucleic acid

DPBS: Dulbecco's phosphate-buffered saline

EGF: epidermal growth factor

EGFP: enhanced green fluorescent protein

EN: endonuclease

FBS: fetal bovine serum

FGF-2: fibroblast growth factor-2

GFAP: glial fibrillary acidic protein

GDNF: glial cell-derived neurotrophic factor

HERV: human endogenous retrovirus

IGF-1: insulin-like growth factor 1

IL-6: interleukin 6

IL-8: interleukin 8

IL-1ß: Interleukin 1 beta

iPSC: induced pluripotent stem cells

KO: knockout

LIF: leukemia inhibitory factor

LINE-1: long interspersed element-1

LTD: long term depression

LTP: long term potentiation

LTR: long terminal repeat

MAP2: microtubule associated protein 2

MeCP2: methyl-CpG binding protein 2

M.O.I: multiplicity of infection

mRNA: messenger RNA

NFIA: nuclear factor A-type

NPC: neural progenitor cells

NT3: neurotrophin-3

NVP: nevirapine, a non-nucleoside reverse-transcriptase inhibitor

ORF: open reading frame

ORF1p: ORF1 protein

ORF2p: ORF2 protein

Pen-Strep: Penicillin-Streptomycin

piRNA: PIWI-interacting small RNA

qPCR: quantitative polymerase chain reaction

RC-L1: retrotransposition-competent L1

RNA: ribonucleic acid

RNP: ribonucleotide particle

RT: reverse-transcriptase

RTi: reverse-transcriptase inhibitor (treatment containing 3TC and d4T)

RTT: Rett syndrome

SYN: synapsin

TE: transposable element

TREX1: three prime repair exonuclease 1

TPRT: target-primed reverse transcription

UTR: untranslated region

VGLUT: vesicular glutamate transporter

LIST OF FIGURES

LIST OF SCHEMATICS

LIST OF TABLES

ACKNOWLEDGEMENTS

I would like to acknowledge Dr. Alysson Muotri for allowing me the opportunity to pursue cutting edge stem cell research. The past two and half years in the Muotri Lab have been integral to my growth as a researcher.

I would also like to thank my committee members Dr. Douglass Forbes and Dr. Stacey Glasgow. Dr. Forbes' class on Cell Biology was one of the most informative classes I took as an undergraduate as it gave me a comprehensive foundation to build off of. Thank you both for your valuable input.

Lastly, I would like to thank Dr. Angela Macia for being an incredible mentor and friend. Prior to working with you, I was unsure of my career goals nor did I understand the rigors and commitment of scientific research. Your guidance and mentorship have made me a more confident scientist and have shown me that I would like to continue a career in translational research. Thank you for the time and effort you have invested in me, I am truly grateful.

ABSTRACT OF THE THESIS

Modeling MeCP2 loss-of-function in human iPSC-derived astrocytes highlights LINE-1 retrotransposon as contributor to neuroinflammation

by

Aurian Saleh

Master of Science in

Biology

University of California San Diego, 2020

Professor Alysson R. Muotri, Chair
Professor Douglass Forbes, Co-Chair

Long interspersed nuclear element-1 (LINE-1) are endogenous, self-propagating genomic sequences that comprise ~17% of the human genome. Retrotransposons play a critical role in genomic and cellular instability, particularly in various forms of human disease. In the diseased state, there is mounting evidence that endogenous retroelements play a role in etiopathogenesis of inflammatory diseases. Mutations in methyl-CpG-binding protein 2 (MeCP2), widely regarded as a global methylator and transcriptional repressor, result in increased LINE-1 expression and activity. Patients with mutations in MeCP2 have subclinical inflammatory phenotypes and cytokine dysregulation. Although *de novo* LINE-1 activity seems to occur frequently in neurons, little is known about the

contribution of this element in glial cells. Astrocytes with mutations in *MECP2* are abnormal in several key functions, thus we sought to investigate astrocyte-mediated inflammation caused by MeCP2 loss-of-function mutations. We generated iPSC-derived astrocytes from MeCP2-KO and healthy controls to observe whether LINE-1, which we know to be upregulated, contributes to the inflammatory phenotype observed. We chronically treated our cells with reverse transcriptase inhibitors (RTi) to reduce endogenous LINE-1 activity. Interestingly, we found upregulation of neuroinflammatory-related genes, increased levels of the proinflammatory cytokine IL-6 as well as an increase in reactive oxygen species, extracellular glutamate and glutathione levels in MeCP2-mutant astrocyte cultures when compared to control cells. Remarkably, inhibition of LINE-1 with RTis improved most of these pathological phenotypes in mutated cells. We hope our work brings further attention to mobile genetic elements, as they contribute more to disease pathologies than previously thought.

INTRODUCTION

1. Transposable elements (TE)

1.1 Classes of TE

Less than 2% of the human genome is protein coding. About 30% is contained within intronic sequences and 45-50% is comprised of repetitive sequences, some of which are capable of mobilizing into novel positions within chromosomes, referred to as transposable elements (TE) (Lander, Linton et al. 2001). These endogenous retroelements have had substantial impact on the evolution of the human genome, ranging from small scale changes induced by insertional mutagenesis to larger scale gene expression changes induced by alterations in splicing and epigenetic modifications (Cordaux and Batzer 2009). Thought to mediate normal neuronal somatic mosaicism in typically developing individuals, retroelements in the diseased state can sustain increased activity and contribute to pathophysiology.

Transposons can be categorized as DNA or RNA transposons. Activity of DNA transposons, also known as Class II transposable elements, no longer contributes to mutagenesis in humans as they are unable to mobilize (Pace and Feschotte 2007). Class I RNA transposons (retrotransposons) are further categorized based on the presence or absence of flanking long terminal repeats (LTR). Retrotransposons use a "copy and paste" mechanism whereby the original sequence is copied via an RNA intermediate and subsequently chaperoned, copied and integrated into a separate location within the genome. Elements such as Mammalian apparent LTR-retrotransposons (MaLR) and human endogenous retroviruses (HERV) both contain LTR sequences that flank internal coding regions (Smit 1993). LTR retrotransposons comprise about 8% of the human genome (Cordaux and Batzer 2009).

Non-LTR retrotransposons are by far the most active TEs during recent human evolution and can be further classified into two subtypes: LINE (Long Interspersed Nuclear Elements) and SINE (Short Interspersed Nuclear Elements) (Lander, Linton et al. 2001, Dewannieux, Esnault et al. 2003).

Together, LINE and SINE comprise ~33% of the human genome (SINEs, including Alu and SVA elements, are non-autonomous sequences transcribed by RNA Polymerase III (Dewannieux, Esnault et al. 2003). Alu sequences are present in over 1 million copies in the human genome while SINE-R/VNTR/Alu (SVA) elements together constitute more than 10% of the human genome (Lander, Linton et al. 2001).

1.2 LINE-1 retrotransposons

LINE-1 elements are ubiquitous, autonomous retrotransposons with an estimated 500,000 copies contained within the human genome (Lander, Linton et al. 2001, Goodier and Kazazian 2008)). A majority of LINE-1 copies are immobile and unable to retrotranspose, due either to 5' truncations or inversions introduced into the sequence (Boissinot, Entezam et al. 2001, Ostertag and Kazazian 2001). Approximately 80-100 copies are mobile (labeled retrotransposition- competent LINE-1 or RC-L1) (Brouha, Schustak et al. 2003).

Full length, RC LINE-1 are 6kb in length and contain a 5' untranslated region (5'UTR), two open reading frames (ORF1, 2), and a 3'UTR followed with a poly-A tract (Swergold 1990). The LINE-1 promoter region has no TATA-box and displays both sense and antisense activity within the 5' UTR (Swergold 1990, Speek 2001). The LINE- 1 ORF1 encodes for a protein that has nucleic acid chaperone activities and an RNA binding domain (Martin and Bushman 2001, Martin, Cruceanu et al. 2005). ORF2 encodes for a protein with enzymatic activity required for LINE-1 retrotransposition. ORF2p has both endonuclease (EN) and reverse transcriptase (RT) activities; equally critical for target site cleavage and integration (Mathias, Scott et al. 1991).

1.3 LINE-1 retrotransposition cycle

LINE-1 transcription begins within the first 100 base pairs of the 5'UTR, (Swergold 1990, Lavie, Maldener et al. 2004). Once transcribed, the full-length capped and polyadenylated LINE-1 mRNA is exported into the cytoplasm where it combines *in cis* with ORF1 and ORF2 proteins to

form a ribonucleoparticle (RNP) complex **(Schematic 1)** reviewed in (Doucet, Hulme et al. 2010, Macia, Blanco-Jimenez et al. 2015, Elbarbary, Lucas et al. 2016). In a more traditional model, the RNA-protein complex can be imported back into the nucleus by a mechanism not fully understood, where target-primed reverse transcription (TPRT) takes place. The RNP complex binds preferentially to an AT rich consensus target (5'TTTT/AA 3' and variants) (Jurka 1997, Cost and Boeke 1998, Monot, Kuciak et al. 2013).

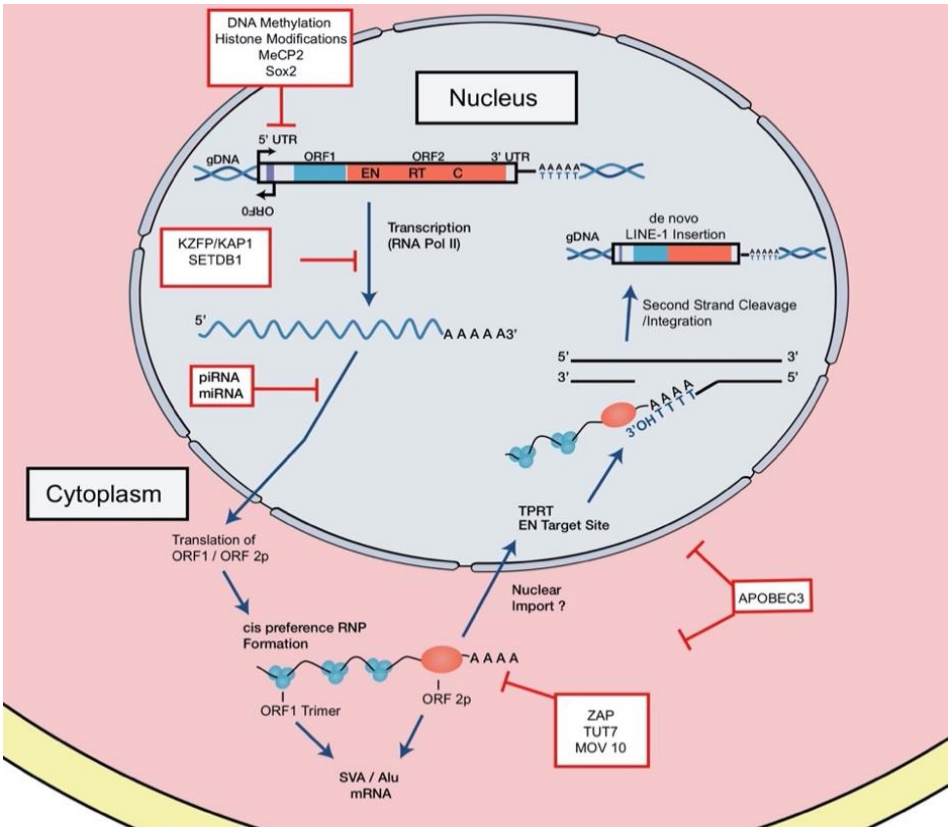

Schematic 1. LINE-1 Retrotransposition Cycle and Host Factor Regulation. RNA polymerase II mediates transcription of retrotransposition-competent LINE-1 sequence. This transcript is exported from the nucleus where it forms an RNP complex with ORF1p and ORF2p. This complex may begin reverse transcription in the cytoplasm. Through a mechanism not well understood, the RNP is imported into the nucleus to begin integration through TPRT. LINE-1 is regulated at distinct intermediates of retrotransposition, indicated in red boxes.

The EN nicks the bottom DNA strand, exposing a 3' OH which primes the reverse transcription of the LINE-1 mRNA template into cDNA (**Schematic 1)**. Recent observations have

suggested that unfinished retrotransposition events may be unable to re-enter the nucleus, accumulating in the cytoplasm, leading to a diseased phenotype (Thomas, Tejwani et al. 2017). The complete mechanism of second DNA strand cleavage and subsequent cDNA synthesis is unknown.

1.4 LINE-1 activity and cellular impact

LINE-1 insertional mutagenesis has resulted in over 120 cases of spontaneous or inherited disease; including diseases such as hemophilia A, cystic fibrosis, and breast cancer; reviewed in (Chen, Stenson et al. 2005). Apart from mutations caused by insertions, DNA recombination of chimeric LINE-1 can lead to large scale structural variation, such as retrotransposition-mediated deletions, duplications, or rearrangements (Gilbert, Lutz-Prigge et al. 2002, Slotkin and Martienssen

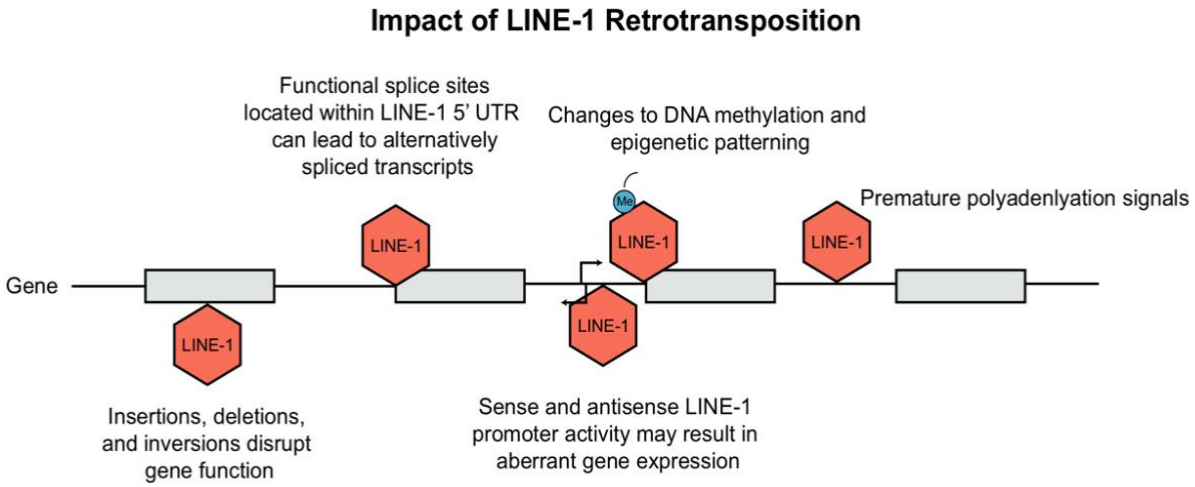

Schematic 2. Consequences of LINE-1 Retrotransposition. Ongoing retrotransposition generates genomic instability and consequently interferes with host gene expression at many levels. Consequences include disruption of gene function due to LINE-1 insertions, as well as generation of mis-spliced or prematurely truncated transcripts. Insertions have been shown to impact host gene expression through changes in epigenetic patterning and LINE-1 promoter activity.

2007).

The presence of both sense and antisense promoter within the 5'UTR of LINE-1 elements can activate upstream or downstream transcription (Nigumann, Redik et al. 2002, Macia, Munoz-Lopez et al. 2011, Elbarbary, Lucas et al. 2016) **(Schematic 2)**. Among all the transcriptionally active

elements present in the human genome, the strength of LINE-1 promoters have been shown to be sequence and context-dependent. Lavie et al. tested various LINE-1 5' UTR constructs to test for observable differences in promoter strength. Although there was no clear link between nucleotide variations and transcriptional activity, deletion of 5' genomic flanking sequences from the constructs resulted in both enhanced and diminished promoter activity, depending on whether the sequence acted as an enhancer or repressor (Lavie, Maldener et al. 2004). In addition to LINE-1 promoters' contribution to aberrant host gene expression, LINE-1 insertions have been shown to create splicing variants; generating either mis-spliced or prematurely truncated transcripts, promoting transcriptional termination or changes to our epigenome by the methylation of LINE-1 CpG islands leading to "epigenetic patterning" and subsequent silencing of neighboring gene promoters (Estecio, Gallegos et al. 2012).

1.5 Cellular response to LINE-1 activity

Given that retrotransposons can impact the cell in a myriad of ways, the host genome has coevolved to employ a variety of responses to repress activity **(Schematic 1)**. Transcriptional repression, in the form of 5-methylcytosine (5mC) and N6-methyladenine (6mA) DNA methylation and repressive histone markers are widely used to regulate TE activity (Hatanaka, Inoue et al. 2015, Deniz, Frost et al. 2019). TE's also harbor binding sites for many transcription factors; the Kruppel-associated box (KRAB)-containing zinc finger proteins (KZFPs) are key regulators of TE activity—often repressing TEs expressed in early embryos (Chuong, Elde et al. 2017, Guo, von Meyenn et al. 2018). LINE-1 activity can be regulated post-transcriptionally by microRNAs (miRNA) and PIWI-interacting RNAs (piRNAs). The role of RNA interference (RNAi) effectors in regulating TE transcripts is substantial; RNA-induced silencing complex (RISC) pathways are common cellular processes that utilize endonucleolytic cleavage to degrade TE transcripts (Yang and Kazazian 2006). If the LINE-1 transcript is not targeted for degradation, the cell will employ other host factors to

target downstream complexes within the retrotransposition cycle. The LINE-1 RNP complex is commonly targeted for degradation and destabilization by various zinc finger and APOBEC enzymes (Kulpa and Moran 2005, Goodier, Zhang et al. 2007, Warkocki, Krawczyk et al. 2018) **(Schematic 1)**. Even with the plethora of host mechanisms put in place to repress endogenous retroelements, *de novo* insertions still take place within somatic tissues, with higher rates of LINE-1 retrotransposition occurring in neural lineages and during development.

1.6 LINE-1 activity during embryogenesis and early brain development

LINE-1 elements are active in germ cells within the testes and ovaries, demonstrating their role in genome evolution, as germline insertions are inherited by progeny (Huang, Burns et al. 2012). **(Schematic 3)** Waves of *hypo*methylation during embryogenesis have been linked with higher rates of retrotransposition; retrotransposition events were shown to occur in embryos pre-implantation onto the uterus (Kano, Godoy et al. 2009).

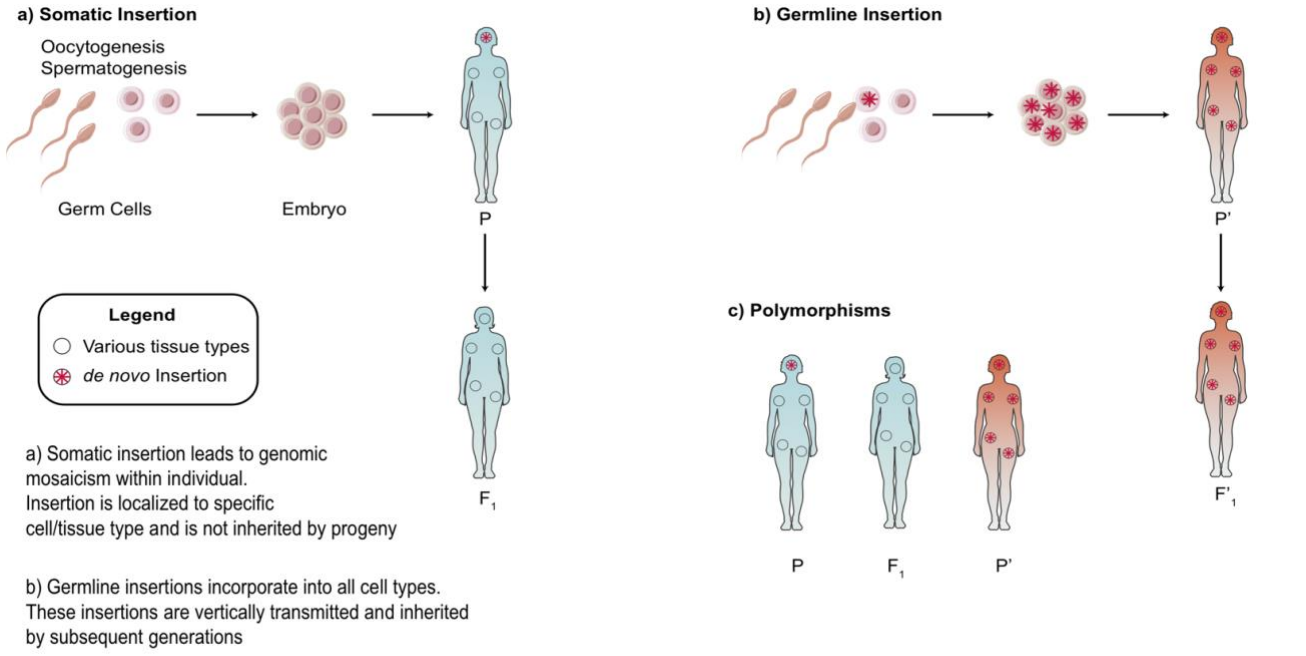

Schematic 3. Somatic vs Germline Insertions. Differences between the heritability of germline vs somatic retrotransposon insertions. **a.** Somatic insertions lead to mosaicism within the individual but are not inherited **b.** Generally, germline or early embryonic insertions are incorporated into the three germ layers and are present in all tissue types. **c.** Example of polymorphisms across different populations based on the presence or absence of an insertion.

Somatic insertions **(Schematic 3)**, on the other hand, occur later in development and are not inherited by progeny. They accumulate over time within an individual and are restricted to the cell or tissue type in which the insertion occurred. This leads to a phenomenon known as somatic mosaicism, whereby large differences in genetic content exist from cell to cell within an individual (Baillie, Barnett et al. 2011). Through the use of an engineered LINE-1 element tagged to a retrotransposition-indicator cassette, retrotransposition events were shown to occur *in vitro* with adult rat neural progenitor cells (NPCs) and in the brains of mice *in vivo*. This was one of the earliest documented cases of somatic retrotransposition occurrence *in vivo* (Muotri, Chu et al. 2005). New retrotransposition events may alter gene expression and ultimately influence cellular phenotype; in the healthy brain this is thought to contribute to neuronal somatic diversification. A few years later, endogenous LINE-1 mRNA was shown to be detectable in NPCs isolated from human fetal brain cells (Coufal, Garcia-Perez et al. 2009). To investigate endogenous LINE-1 activity, a copy number variant (CNV)-based qPCR assay was performed on genomic DNA extracted from various tissue types of healthy human adults. Interestingly, it was reported that ORF2 content in the hippocampus was consistently higher when compared to heart or liver samples from the same individual (Coufal, Garcia-Perez et al. 2009). The hippocampus, being one of the few brain regions consisting of a neurogenic niche, is ubiquitous with genomic LINE-1 mosaicism. Because LINE-1 retrotransposition events have increased occurrence during neurogenesis (Muotri, Chu et al. 2005, Salvador-Palomeque, Sanchez-Luque et al. 2019), it is likely that LINE-1 activity rises in a region like the hippocampus (Coufal, Garcia-Perez et al. 2009). A recent analysis of 24 hippocampal neurons using RC-seq, whole genome sequencing (WGS), and LINE-1 insertion profiling revealed that somatic insertions which occur during neurodifferentiation in hESCs may occur due to mutations at the Ying Yang 1 (YY1) transcription factor binding site (Sanchez-Luque, Kempen et al. 2019). Retrotransposition events occurring during neural development may contribute to “genome

plasticity" and neuronal diversity by allowing for variations in genomic DNA from cell to cell.

1.7 Retrotransposons and Inflammatory Disease Phenotypes

Intrinsic immune responses to viral pathogens are co-opted to restrict retroviruses and retrotransposons as well. Endogenous transposon activity can elicit the same interferon responses that are associated with retroviral infections (Crow 2010, Chuong, Elde et al. 2016). Accumulation of endogenous nucleic acids in the cytoplasm can induce activation of toll-like receptors and type I interferon proteins (IFN) (Crow and Rehwinkel 2009, Crow 2010) Similarly, when viral DNA is present in the cytoplasm, it triggers activation of the cGAS (cyclic GMP-AMP synthase)/STING (stimulator of interferon genes) pathway, resulting in an interferon-mediated response.

Endogenous retroelements have been linked as key effectors of inflammation in various autoimmune and neurodegenerative disorders, reviewed in (Saleh, Macia et al. 2019). This can be seen in the case of Aicardi-Goutieres syndrome (AGS), which features a progressive inflammatory encephalopathy, resulting in severe mental and physical handicap as well as greatly reduced lifespan. AGS can result from mutations in the antiviral enzyme three-prime repair exonuclease 1 (TREX1), which functions to cleave nucleic acids in the cytosol. In TREX-1 deficient NPCs, neurons and astrocytes, single-stranded DNA (ssDNA) species in the cytosol were demonstrated to be significantly increased. Sequencing data suggests that most of the ssDNA found was derived from *cis* LINE-1 reverse transcription (Thomas, Tejwani et al. 2017). This is correlated with higher expression of IFN-α in astrocytes, which was reduced to near control levels with chronic treatment of reverse transcriptase inhibitors (RTis).

Similarly, LINE-1 was demonstrated to contribute to age-associated-inflammation, due to a failure of host surveillance mechanisms in senescent cells (De Cecco, Ito et al. 2019). Cellular senescence was associated with downregulation of LINE-1 surveillance factors such as TREX1 and RB-1 (Retino-blastoma transcriptional corepressor-1). Loss of TREX-1 comprised the removal of

cytoplasmic LINE-1 DNA while loss of RB-1 relieved heterochromatin repression. Increased LINE-1 copies in the cytoplasm triggered IFN-I response, a phenotype that improved with inhibition of LINE-1 RT (De Cecco, Ito et al. 2019). Elevated LINE-1 copies in human cells can modulate cellular phenotypes and contribute to inflammation-related pathologies. There is mounting evidence that endogenous retroelements play a large role in initiating neuroinflammation. This has been shown to occur through a variety of mechanisms, generally involving context-specific derepression of LINE-1 activity. Consequently, we wondered whether LINE-1 elements engage the pathophysiological pathways leading to features of the disease pathology.

2. Methyl-CpG Binding Protein 2 (MeCP2*)* and LINE-1

2.1 Human Diseases associated with MeCP2

One of the main forms of LINE-1 inhibition occurs through transcriptional-mediated repression. MeCP2 binds to methylated CpG islands within the LINE-1 5' UTR, recruits various scaffolding proteins to induce chromatin remodeling. When *MECP2* is mutated, LINE-1 activity and expression is increased in the brain (Muotri, Marchetto et al. 2010). *De novo* mutations in the X-linked gene *MECP2* are strongly linked to Rett Syndrome (RTT). RTT a severe progressive neurological disorder with no known cure and an incidence of 1 in 10,000 to 1 in 15,000 females. Individuals with mutations in the *MECP2* gene results in a mosaic of symptoms and symptom severities in affected females due to MeCP2 dosage compensation through X chromosome inactivation (Amir et al., 1999).

Although recently removed from the umbrella of Autism Spectrum Disorders (ASD), patients with RTT display autistic phenotypes such as early infantile hypotonia and profound psychomotor delays including a regression of language and motor skills (Zhao, Wu et al. 2019). Symptoms may also include microcephaly, epilepsy and apraxia. Progressive microcephaly is a classic clinical

feature for patients with Rett (Ahmed 2007). The decrease in brain volume is associated with abnormally small neurons containing less complex dendritic branching, all densely packed together (Armstrong, Dunn et al. 1995). Brain volume was shown to be selectively reduced in the parietal and temporal lobes of RTT patients (Carter, Lanham et al. 2008). Indeed, cortical dendritic spines, which transmit excitatory glutamatergic input into electrical signals, are reduced in number and density in Mecp2 null mice (Belichenko, Wright et al. 2009) leading to deficits in synaptic contacts. Mutations in *MECP2* are not only linked to RTT, but also to multiple neurological diseases such as Huntington's disease, Autism, Angelman Syndrome, as well as non-neurological diseases such as breast and liver cancer (Ezeonwuka and Rastegar 2014). The widespread and diverse function of MeCP2 underscores its role in many disorders.

2.2 *MECP2* gene and function

MeCP2 is a multifunctional nuclear protein with two functional domains: a methyl DNA binding domain and a transcription repression domain (Chahrour, Jung et al. 2008, Hite, Adams et al. 2009). This protein modulates neuronal chromatin architecture and organization; once bound to methylated CpG islands, it recruits a variety of interacting machinery such as various histone deacetylases and methyltransferases (Martinez de Paz and Ausio 2017). *MECP2* is widely regarded as a global histone methylator and transcriptional repressor, however, it has been shown to associate with transcriptional activators and so functions as both an activator and repressor of transcription. *MECP2* RNA is present in all mouse and human tissues, and is highly expressed in the brain when compared to other tissues (https://www.proteinatlas.org/ENSG00000169057-MECP2/tissue). It is not fully understood how *MECP2* functions at a cellular level; one murine study mapped neuronal Mecp2 binding sites via ChIP-chip analysis and found a majority of the promoters which bound Mecp2 were on active genes, not silenced ones, as one would expect (Chahrour, Jung et al. 2008). Interestingly, many *MECP2* binding sites were found in intronic regions outside of transcription

units (Yasui, Peddada et al. 2007). MeCP2 is localized to both synaptic terminals and the nucleus and acts on multiple loci, suggesting that its mis regulation can affect multiple molecular and signal transduction pathways (Aber, Nori et al. 2003).

MeCP2 is a multifunctional epigenetic regulator that can induce transcriptional repression, activation, chromatin remodeling and RNA splicing (Young, Hong et al. 2005, Nikitina, Shi et al. 2007, Yasui, Peddada et al. 2007). As mentioned previously, the widespread and diverse epigenetic processes of MeCP2 emphasize its role in many disorders. In the next section, we address how *MECP2* mutations effect LINE-1 expression.

2.3 MeCP2 loss of function and LINE-1

MeCP2 loss of function increases susceptibility for LINE-1 mobilization because the promoter region within the LINE-1 5'UTR are targets of MeCP2-mediated transcriptional repression (Muotri, Marchetto et al. 2010). Post-mortem brain tissue from patients with RTT show higher genomic LINE-1 ORF2 sequences when compared to controls (Muotri, Marchetto et al. 2010). *In vivo* experiments performed on transgenic mice containing a human LINE-1-eGFP reporter cassette, illustrates that Mecp2-KO mice display on average, a 3.5 fold increase EGFP positive cells in regions such as the cerebellum, striatum, cortex, and hippocampus (Moran, Holmes et al. 1996, Muotri, Marchetto et al. 2010). This trend is CNS-specific as LINE-1 copy numbers are not significantly increased in fibroblast cells isolated from Mecp2-KO mice.

LINE-1 retrotransposition, which we know to be modulated by *MECP2* and upregulated in MECP2-KO cells, has been shown to contribute to morphological and synaptogenic deficits in patient iPSC-derived neurons (unpublished data). Chronic treatment of nucleoside analogs, which efficiently inhibit LINE-1 reverse transcriptase activity, lead to a rescue of neural morphology, synaptogenesis, and partial rescue of spontaneous neural activity defects. In addition, the observed microcephalic-like reduction in RTT 3D cortical organoids was significantly rescued with RTi

treatment. These drugs have huge therapeutic potential not only in RTT, but also in other disorders where endogenous retroelements are mis regulated. In fact, there are clinical trials currently underway utilizing RTi therapy for disorders such as AGS or ALS (amyotrophic lateral sclerosis) patients.

2.4 Astrocyte Influence in MECP2-deficient cells

It is becoming increasingly evident that under pathological conditions, there is a non-cell autonomous effect in the CNS, in which glial cells are as vulnerable as neurons (Okabe, Takahashi et al. 2012, Serio, Bilican et al. 2013, Song, Feodorova et al. 2014, Williams, Zhong et al. 2014, Russo, Freitas et al. 2018). The effect of *MECP2* mutations on astrocyte function is profound. The extent to which astrocytes, the most abundant cell type in the CNS, can contribute to the pathology of the disease has been studied (Maezawa, Swanberg et al. 2009, Lioy, Garg et al. 2011, Delepine, Meziane et al. 2016, Dong, Liu et al. 2018). When Mecp2 is restored to astrocytes in otherwise null mice, there is a delay in the progression of disease phenotypes. Specifically, there are significant improvements to locomotion and anxiety levels as well as a prolonged lifespan (Lioy, Garg et al. 2011). Mecp2-expressing astrocytes were also shown to exert a non-cell autonomous effect on neighboring neurons, increasing dendritic branching and levels of transporter VGLUT, involved in excitatory neurotransmission (Lioy et al., 2011). Even more, mutant astrocytes were shown to negatively influence MeCP2 expression in neighboring cells, in part through intercellular gap junctions (Maezawa, Swanberg et al. 2009, Williams, Zhong et al. 2014). From a functional standpoint, it was shown that MeCP2 mutant astrocytes display abnormal spontaneous oscillations in cytoplasmic Ca^{2+}. These cells show higher frequencies and peak amplitudes than wildtype astrocytes. Mechanistically, this was linked to abnormal Ca^{2+} load in the endoplasmic recticulum, resulting in leaking Ca^{2+} and excessive activation of NMDA receptors on neighboring neurons (Dong, Liu et al. 2018).

Accumulating evidence links the cytokine dysregulation and persistent inflammatory phenotypes seen in mice and iPSC-derived models with astrocyte functional abnormalities (Cortelazzo, De Felice et al. 2014, Colombo and Farina 2016, Cortelazzo, De Felice et al. 2017)**.** Astrocytes are key mediators of neuroinflammation, either through exacerbating inflammatory reactions or promoting immunosuppression and tissue repair (Serio, Bilican et al. 2013, Colombo and Farina 2016). Patients with mutations in *MECP2* display subclinical inflammation profiles and dysregulation of chemokine and cytokine expression (Cortelazzo, De Felice et al. 2014, Cortelazzo, De Felice et al. 2017). Evidence supports immunological defects and immunodeficiency in patients, resulting from mis regulated internal inflammatory responses (van der Vaart, Svoboda et al. 2017).

We consistently see an activation of retroelements in the diseased state and more prominently in cases of neurodegenerative disease. It is not fully understood how this is initiated or whether it directly contributes to disease pathology. Recent studies have demonstrated that in the diseased state, LINE-1 activity is derepressed, which can lead to accumulation of cytoplasmic LINE-1 DNA (**Schematic 4**). This triggers various innate immune responses such as interferon-mediated inflammation (Thomas, Tejwani et al. 2017, De Cecco, Ito et al. 2019, Simon, Van Meter et al. 2019, Tharp, Malki et al. 2020). Although *de novo* LINE-1 insertions seem to occur frequently in neurons, little is known about the contribution of this element in glial cells (Singer, McConnell et al. 2010, Upton, Gerhardt et al. 2015).

For this thesis, we sought to investigate astrocyte mediated inflammation in MeCP2 loss-of-function mutations through treatments with reverse- transcriptase inhibitors (RTis). Thus, using human iPSC derived astrocytes as a model, we generated control (CTRL) and MECP2-KO astrocytes to observe whether LINE-1, which we know to be upregulated, contributes to the inflammatory

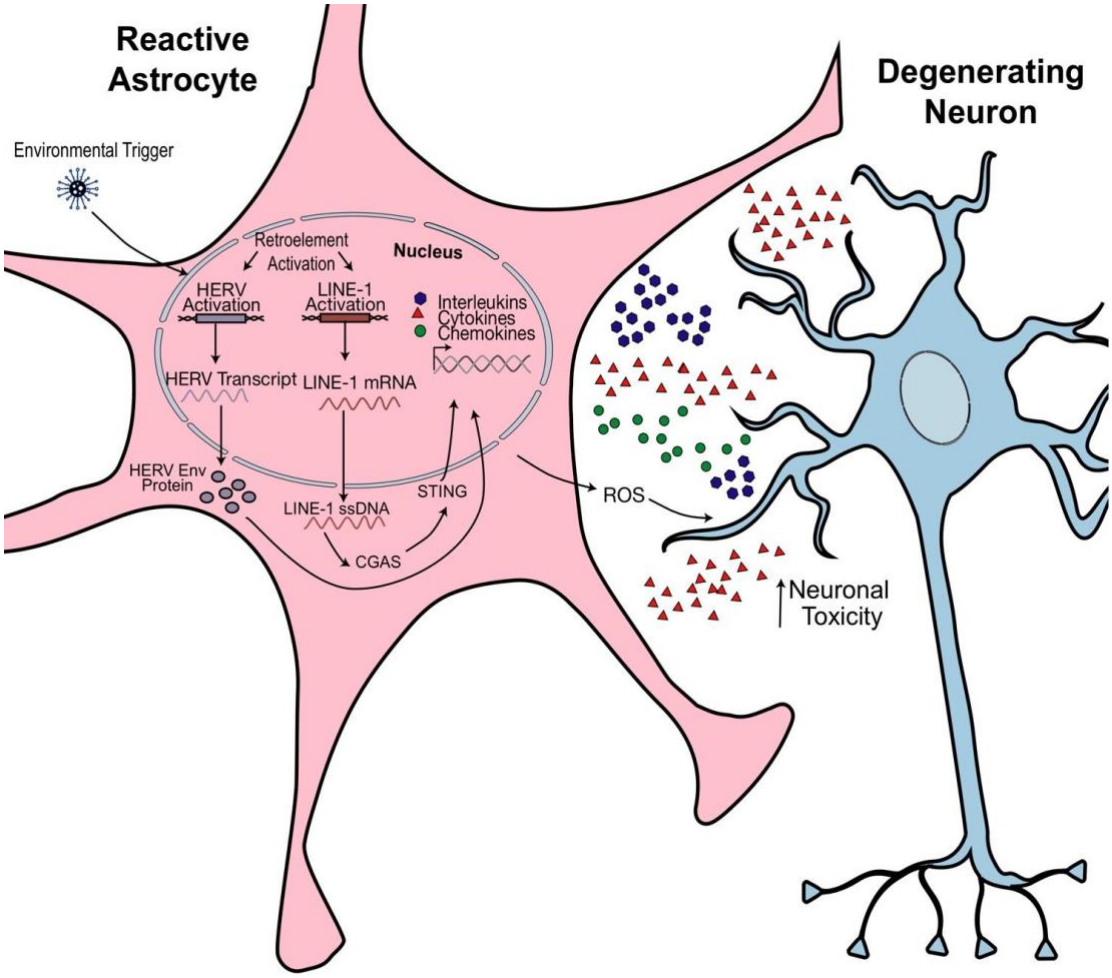

Schematic 4. Hypothesized Model of Retroelement-mediated Neuroinflammation. Environmental or cellular triggers may activate retrotransposon transcription. Production of pathogenic HERV Envelope proteins (Env) or cytoplasmic accumulation of LINE-1 ssDNA activates an innate immune response. Astrocytes become activated, releasing proinflammatory cytokines and reactive oxidative species (ROS). This has toxic effects on neighboring neurons and could promote morphological and synaptogenic defects, subsequently promoting neuropathophysiological effects.

phenotype observed in MeCP2-deficient astrocytes. We also asked whether astrocyte-related pathologies could be reduced by inhibiting LINE-1 elements. We report significant dysregulation of genes involved in interleukin signaling, toll-like receptor signaling and cytoplasmic DNA sensing pathways between CTRL and MECP2-KO astrocytes. We then examined the effects of this mutation

downstream by looking at cytokine release and extracellular glutamate levels. Additionally, we took measures of astrocyte oxidative stress with assays measuring glutathione and ROS (reactive oxidative species) levels. We find significant improvements to gene expression and downstream responses in astrocytes treated with RTis. These results indicate that LINE-1 activation contributes to the pathologies observed in MECP2-KO astrocytes. We hope these results bring more attention mobile genetic elements, as they play a larger role in initiating disease pathogenesis than previously thought.

MATERIALS AND METHODS

Patient consent

Informed consent was obtained from patients who donated control (CTRL) and MECP2-KO fibroblasts. Fibroblasts were collected from dermal biopsies under protocols approved by the University of California, San Diego Institutional Review Board (#141223ZF).

Astrocyte Generation

iPSCs were differentiated into NPCs as described in (Marchetto, Carromeu et al. 2010). NPCs were cultured on 20 µg/mL poly-L-ornithine (Sigma-Aldrich, P3655) and 5 µg/mL laminin (Life Technologies, 23017015) coated plates and seeded at a density of 1.6 million cells per 100mmx20mm plates (Corning, 430167). Media was changed every other day with NG medium (DMEM/F12 50/50 1X (Gibco 11330-032), 0.5% penicillin/streptomycin (Life Technologies, 15140163), 1 % N2 NeuroPlex (Gemini Bio-Products, 400163) and 1% SM1 (StemCell, 05711) supplemented with 20 ng/mL human fibroblast growth factor basic (bFGF) (R&D Systems, 414-TE). For differentiation into neurons, the bFGF was withdrawn from the NG media and Rock inhibitor (Y27632) was added at a concentration of 10ng/mL for 48 hours; cells matured and remained in culture for 6-9 weeks.

Astrocyte differentiation was followed as described in (Serio, Bilican et al. 2013). Monolayer NPCs were dissociated into single cell suspension using StemPro Accutase (Life Technologies, A1110501). To form astrospheres, cells were seeded at density of 4-5 million cells per well in a 6-well plate (Genesee, 25-105) shaking at 95 r.p.m. at 37˚C in NSCR EL medium containing DMEM/F12 (Gibco) with 1% N2 supplement (Gibco) and 0.1% SM1 supplement, 1% nonessential amino acids (Gibco 11140-050), 1% penicillin/streptomycin (Gibco, 15140-122), 1% GlutaMAX solution (Gibco, 35050-061), 20 ng/mL EGF (Peprotech AF-100-15-1MG) and 20 ng/mL LIF (Peprotech 3000-05). Following 2-4 weeks in the NSCR EL media, the astrospheres

were expanded in NSCR media now supplemented with 20 ng/mL EGF and 20 ng/mL FGF (NSCR EF) for 2-4 weeks.

Following this expansion phase, astrospheres were plated on 20 µg/mL poly-L-ornithine and 5 µg/mL laminin and remained in NSCR EF media allowing astrocyte progenitor cells to migrate outward until 70% confluency. For astrocyte assays, progenitors were passaged and seeded at 50,000 cells/well in a 96 well plate. For differentiation into mature astrocytes, media was changed to contain half of the NSCR basal media and half Astromed CNTF media. Astromed media contained Neurobasal media (Gibco) with 0.2% SM1, 1% NEAA, 1% penicillin/streptomycin, 1% Glutamax supplemented with 10ng/mL CNTF (Peprotech 450-13). After 48hrs, cells were transitioned into full Astromed CNTF media for 14 days. Media was conditioned for 48 hours prior to assays.

RTi preparation

The reverse-transcriptase inhibitors were prepared as follows: Lamivudine (3TC, Sigma-Aldrich, L1295) was prepared in dimethyl sulfoxide (DMSO, Sigma Aldrich, D2650) and 10 µM of 3TC was used in media. Stavudine (d4T, Sigma-Aldrich, D1413) was re-suspended in water and 1µM of d4T was used in media in combination with 3TC. Nevirapine (Sigma Aldrich, SML0097) was re- suspended in DMSO and 400nM nevirapine was used in media. CTRL cells contained 10 µM of DMSO as a vehicular control.

RNA extraction

RNA was extracted by using RNAse Plus Mini Kit (Qiagen). Briefly, adherent cells were washed with DPBS and further lysed using RLT buffer with b-mercaptoethanol and dissociated using a 1mL syringe (Fisher Scientific, 1482330) and a needle (VWR, BD- 305196). RNA from lysates was extracted following manufacturer's instructions. cDNA was generated using the Qiagen

Quantitect Reverse Transcription Kit.

PCR array

PCR array was performed by using RT_2 Profiler PCR Array 384 format (Qiagen), following manufacturer's instructions. Briefly, 400ng of total RNA was used for reverse transcription by using the RT_2 First Strand Kit (Qiagen). Genomic DNA was eliminated prior to reverse transcription. Real-Time PCR was performed by using RT_2 SYBR Green Mastermix and cDNA mix, divided into 384 wells. Plates were sealed with Optical Adhesive Film and run into a CFX384 (BioRad). Run conditions: 1 cycle of 10 min at 95ºC, followed by 40 cycles of 15s at 95ºC and 1 minute at 60ºC, where data collection was performed. For data analysis, GeneGlobe Data Analysis Center was used.

Extrachromosomal DNA extraction and LINE-1 qPCR

Extrachromosomal DNA was extracted from 7w old neurons using Modified Hirt protocol described previously (Arad 1998). Neurons (10_6) were washed with Ca^{2+} and Mg^{2+} free phosphate buffered saline and dissociated with Accutase at 37C for 20-30 minutes. Samples were counted with Via-1 cell counter and pelleted. Pellets were resuspended in Buffer 1 (50mM Tris-HCl, 10mM EDTA, supplemented with 100 μg/mL RNase A. Cells were lysed with Buffer 2 (1.2% SDS) and inverted to mix. High molecular weight chromosomal DNA was precipitated with Buffer 3 (3M CsCl, 1M potassium acetate, and 0.67M acetic acid). The resultant supernatant was column purified following the ssDNA protocol (Macherey-Nagel 740609.250) qPCR was run with the following LINE-1 probes. We generated a standard curve to extrapolate absolute number of copies with given Ct. Both were normalized relative to their own internal control.

ORF1 –
ATGGGGAAAAAACAGAACAGAAAAACTGGAAACTCTAAAACGCAGAGCGCCT
CTCCTCCTCCAAAGGAACGCAGTTCCTC

ORF2 –
GCTCATGGGTAGGAAGAATCAATATCGTGAAAATGGCCATACTGCCCAAGGTA
ATTTACAGATTCAATGCCATCCCCATC

ORF2-3′UTR –
TGGAAACCATCATTCTCAGTAAACTATCGCAAGAACAAAAAACCAAACACCGC
ATATTCTCACTCATAGGTGGGAATTGA

Immunofluorescence

For adherent cells, cells were washed with DPBS, fixed in 4% paraformaldehyde (PFA, Core Bio, 19943) for 20 minutes at room temperature. For IF, cells were permeabilized with 0.1% Triton X-100 (Promega, H5142) for 10 minutes at room temperature. Cells were placed in a blocking solution (DPBS, 10% donkey or goat serum (Fisher Scientific, 50413115, 50413116), and 0.005% Triton X-100) and incubated for 30 minutes at room temperature.

Primary and secondary antibodies were diluted in solution containing DPBS, 1% donkey or goat serum, and 0.005% Triton X-100. Cells were incubated with the primary antibody overnight at 4˚C. The next day, cells were washed with DPBS three times for 5 minutes and incubated with primary antibody: overnight. Cells were washed 2X with DPBS and secondary antibody was incubated for 30 min at room temperature. After 2X wash with PBS, DAPI was added (VWR International, 80051-386, 1:10,000) for 10 minutes at room temperature. Prolong Gold antifade mountant (Life Technologies, P36930) was added to preserve fluorophore intensity.

Primary antibody dilutions are as followed: anti-GFAP (1:1000) (ab4674), anti-S100B (1:500) (ab868), anti-MAP2 (ab5392) (1:1000), anti-NF1A (1:1000) (ab228897), anti-Vimentin 1:100 (Invitrogen OMA106001)

Secondary antibodies conjugated to Alexa Fluor 488, 555, and 647 were diluted 1:1000 (Life Technologies).

IL-6 ELISA

Following 14 days of differentiation, astrocyte media was conditioned for 48 hours and tested for presence of IL-6 without exogenous stimulation (R&D Systems D6050). All samples were assayed in triplicate following the cell culture supernatant protocol. To observe functionality of astrocytes, cells were stimulated with 10ng/ml of proinflammatory cytokine IL-1β for 48 hours and resultant media was assayed, and corresponding plate was fixed and stained for normalization. Optical density was measured at 450nm with wavelength correction set to 540nm using Tecan Infinite Pro 200 plate reader. Standards were assayed in duplicates and samples were assayed in triplicates. Values were normalized to number of GFAP+ cells. About 8-10 images were taken per condition and counted using Image J.

Glutamate Assay

Medium from astrocytes differentiated for 14 days with CNTF was conditioned for 48 hours. Glutamate assay (ab83389) was specific to detect levels of glutamate not glutamine or glutamic acid. The "Serum/urine" protocol was followed for cell culture supernatant samples. Extracellular concentrations of glutamate were extrapolated from a standard curve.

ROS Assay

Astrocyte progenitors were plated at a density of 50,000 cells/ well in a white-walled, clear bottomed 96 well plate (Corning) and differentiated for 14 days with CNTF. ROS-Glo H_2O_2 (Promega G8820) Homogenous Lytic protocol was followed according to manufacturer's instructions. Astrocytes and RTi treatments were conditioned in the Astromed media for 48 hours. The H_2O_2 substrate solution was added to the plate and treated for 4 hours before ROS Glo detection solution was added. Relative luminescence was recorded using Tecan Infinite Pro 200

plate reader. Six replicates were run per condition. n=3/4

Glutathione Assay

GSH-GLO Glutathione Assay (Promega V6911) protocol for adherent mammalian cells was followed according to manufacturer's instructions on D14 astrocytes to measure glutathione levels present in astroglial cells. Cells were seeded at 50000 cells/well on a white-walled 96 well plate. Medium was removed from multiwell plate and 1X GSH-Glo reagent was added and incubated for 30 minutes at room temperature. Following addition of Luciferin Detection reagent, relative luminescence was recorded using Tecan Infinite Pro 200 luminometer. Values were normalized to GFAP+ expressing cells.

Ca^{2+} Flux Assay

Rhod-4 No Wash Calcium Assay Kit was performed following manufacturer's instructions. iPSCs-derived neurons were grown a in 96-well plate and cultured in NG media. Media was changed 48 hours prior to the experiment.100ul of Rhod-4 Dye-Loading Solution was added per well and incubated at room temperature for 1hour. Calcium flux assay was run by monitoring the fluorescence intensity at Ex/Em = 540/590 nm. Images were acquired for 20 seconds (approximately 600 frames) per field. For analysis, calcium fluorescence traces were retrieved using customized software, Netcal (Orlandi et al., 2017) based on MatLab software®. First, a manual selection of Regions of Interest (ROIs) was carried out to track the activity of all the cells in the culture, both neurons and astrocytes. After analyzing the recording, further post-processing allow the division of the traces in 2 groups with different firing behavior: neurons that display sharp and fast increase of fluorescence followed by a rapid decline in the wave function, astrocytes that have a slow progression in the florescence intensity and a similar slow decrease in intensity. The classification of the traces was done training

Netcal program with the same parameters for each experiment. The analysis of each group highlights specific characteristics that all the traces in the group share together: Average fluorescence trace, Average number of bursts, Burst intensity and Duration of bursts

Statistical Analysis

Technical replicates were used to determine standard error. N is displayed in each figure legend. Microsoft Excel was used to organize data. Error bars for figures are standard error of the mean (S.E.M.) using GraphPad Prism v7 (Graphpad Software Inc. version 7.0). For t-test analysis, two-tailed unpaired tests with a = 0.05 was used. For multiple comparisons, significance was determined with ANOVA, using Tukey's multiple comparisons test. Grabbs' test with a = 0.05 was performed to determine outliers, and significant values were excluded from analysis.

RESULTS

RTi treatment reduces cytoplasmic LINE-1 DNA in MECP2-KO neurons and increases the number of GFAP expressing cells in MECP2-KO astrocytes.

The cells used in this thesis are derived from fibroblasts from a male patient with a *de novo* mutation in the methyl-CpG binding domain within Exon 3 of the methyl-CpG binding protein 2 (*MECP2)* gene. This results in a nonsense point- mutation altering a glutamine reside to a premature stop codon (Q83X), resulting truncated, non-functional protein (MECP2-KO). Control cells (CTRL) were obtained using the respective father (Zhang, Freitas et al. 2016, de Souza, Carromeu et al. 2017).

Mutations in MeCP2 result in widespread clinical symptoms and severities due to its high expression in most cell types within the brain and role as a global epigenetic regulator (Ezeonwuka and Rastegar 2014). MeCP2 has been demonstrated to mediate transcriptional repression of LINE-1 elements (Muotri, Marchetto et al. 2010). MeCP2 mutant neurons were confirmed to have elevated levels of LINE-1 ORF 2 transcript as well as an increase in endogenous copy number within the genomic DNA in accordance with previous research. Recent studies have linked diseased states with accumulation of cytoplasmic LINE-1 cDNA and interferon-mediated inflammation (Thomas, Tejwani et al. 2017, De Cecco, Ito et al. 2019, Simon, Van Meter et al. 2019, Tharp, Malki et al. 2020). This is due to activation of innate immune components that respond to the presence of cytosolic DNA, such as various cGAS (cyclic GMP-AMP synthase) /STING (stimulator of interferon genes) proteins. Thus, we wanted to investigate whether the lack of MeCP2 in our cells would result not only in an increase of LINE-1 mRNA, but also in an accumulation of LINE-1 cytoplasmic DNA. We generated iPSC-derived neurons from CTRL and MECP2-KO cells as previously described (Marchetto, Carromeu et al. 2010). Extrachromosomal DNA was extracted and purified using a modified HIRT protocol previously

described (Arad 1998). We detected elevated levels of LINE-1 Hs species in the extrachromosomal fraction of MECP2-KO neurons when compared to CTRL neurons (**Fig 1a.)** We report significantly higher levels of LINE-1 ORF1 and ORF2 cytoplasmic DNA in the mutant neurons. The LINE-1 reverse transcriptase (RT) was targeted using a combination of reverse transcriptase inhibitors. Lamivudine (3TC) and Stavudine (d4T) are nucleoside analog reverse-transcriptase inhibitors that have been shown to prevent LINE-1 reverse transcription; while Nevirapine (NVP) is a non-nucleoside analog reverse-transcriptase inhibitor that has been demonstrated to have no effect on LINE-1 reverse transcriptase (Dai, Huang et al. 2011). DMSO was used as a vehicular control. Chronic RTi (3TC + d4T) treatment partially decreased ORF1 cytoplasmic copies while significantly reducing ORF2 copies **(Fig 1a).** These results indicate that cells lacking MeCP2 LINE-1 species are accumulated in the extrachromosomal fraction that can be controlled by the use of inhibitors of LINE-1 reverse transcription.

Due to the findings of previous studies, which link LINE cytoplasmic DNA accumulation as contributors to inflammation, as well as reports that link cytokine dysregulation and persistent inflammatory phenotypes with astrocyte functional abnormalities, we sought to investigate the role of LINE-1 in MECP2-KO astrocytes (Cortelazzo, De Felice et al. 2014, Thomas, Tejwani et al. 2017, De Cecco, Ito et al. 2019). We generated iPSC-derived astrocytes with multiple clones from CTRL and MECP2-KO cell lines (Serio, Bilican et al. 2013). NPCs were cultured in suspension in media containing epidermal growth factor (EGF) and leukemia inhibitory factory (LIF) for 2-4w **(Fig 1b).** Both factors have been shown to increase glial fate specification in the absence of fibroblast growth factor (FGF) or fetal bovine serum (FBS) (Namihira, Kohyama et al. 2009, Sanalkumar, Vidyanand et al. 2010). Following this enrichment phase, the cells are expanded in medium containing EGF and FGF for 2w. The spheres were plated and propagated as monolayer culture for 2 w, with progenitors growing radially from the sphere **(Fig 1b)**. APCs

were differentiated in media containing ciliary derived neurotropic factor (CNTF) for 14d to form GFAP+, S100B+, MAP2- astrocytes **(Fig 1c).** Across multiple rounds of differentiation there was an observable difference in the number of GFAP + astrocytes across the different genotypes. When quantified, we found a significant decrease in the number of GFAP+ cells from the MECP2-KO genotype when compared to CTRL. Interestingly, chronic RTi treatment significantly increased the number of GFAP expressing cells **(Fig 1d)**. This data suggests that treatment with RTi resulted in increased differentiation efficiency into GFAP+ cells.

Genes involved in cytokine expression and innate immunity are upregulated in mutant astrocytes and decreased with RTi and NVP treatment.

There is increasing evidence that immune dysregulation may play a role in the development of RTT (Cortelazzo et al., 2014; Leoncini et al., 2015; Pecorelli et al., 2016), with evidence of altered cytokine levels in blood/plasma, and significant correlations between levels of several specific cytokines and clinical severity. Thus, we performed gene expression analysis in CTRL and MECP2-KO astrocytes to investigate inflammation signatures with and without RTi treatment. We performed a PCR array were 96 genes related to inflammation, immunity, apoptosis and cell differentiation markers were evaluated (see **Table 1** for a full list of genes). When we compared the gene expression signature of MECP2-KO vs CTRL astrocytes, 30 genes were differentially expressed at least two-fold. Various cytokines, interferons, and chemokine receptors such as IL-6 and CXCR2, CCL2, CXCL10 were all significantly upregulated in MECP2 KO astrocytes when compared to CTRL cells **(Fig 2e-h and Fig S1).** Volcano plots show the spread of differentially expressed genes **(Fig 2a)**. Chronic treatment with RTi significantly decrease the expression of upregulated transcripts and the number of differentially expressed genes **(Fig 2b).** Interestingly, we observe a 39-fold increase in expression of TMEM173, a stimulator of interferon protein that detects cytosolic DNA and promotes production of type I interferon (IFN-I) innate immune

response. Inhibition of LINE-1 RT significantly reduces the levels of this transcript in MECP2-KO astrocytes **(Fig. 2e and Fig S1).** Suppressor of cytokine signaling (SOCS1) was also upregulated in mutant astrocytes with significantly reduced expression in RTi treatment **(Fig. 2h)**. NVP treatment also reduces the number of differentially expressed transcripts but to a lesser extent **(Fig 2c).** We then sought to explore which biological processes and pathways were associated with the dysregulated genes using enrichment analysis in multiple databases. Databases Panter 2016 and BioPlanet 2019 identified similar processes including pathways involved in cytokine-cytokine receptor interactions, JAK/STAT signaling, cytosolic DNA sensing pathways as well as interleukin and toll-like receptor signaling **(Fig 2d)**. This data suggests that LINE-1 activation, induced by lack of MeCP2, results in aberrant cytokine and immune signaling in astrocytes. Whether these changes in gene expression alter astrocyte functionality is explored in the next section.

RTi treatment reduces IL-6 cytokine levels in astrocyte conditioned medium.

Following the gene expression data, we performed a variety of functional assays to observe the role LINE-1 elements on astrocyte inflammation processes. Astrocytes are proven to be important players in the in the pathology of many neurodegenerative disorders such as Alzheimer and Parkinson's Disease (Maragakis and Rothstein 2006, Colombo and Farina 2016, Kery, Chen et al. 2020). Excessive activation from astrocytes can cause neurotoxicity and progression of inflammation associated phenotypes. Thus, we aimed to investigate if the activation of LINE-1 elements contributes to a cytokine dysregulation at the protein level in MECP2-KO astrocytes, leading to a neurotoxic phenotype. We performed an ELISA (enzyme-linked immunosorbent assay) designed to detect levels of the proinflammatory cytokine IL-6 in the cell culture supernatant 48 hours after the last media change. We found a six-fold increase in IL-6 levels in medium conditioned from MeCP2-KO astrocytes. Although not statistically significant, chronic

treatment with RTi partially decreases IL-6 levels **(Fig. 3a**). These results suggest LINE-1 activation as a potential contributor to astrocyte mediated cytokine release, but further analysis is needed to reach a comprehensive understanding.

RTi treatment rescues extracellular glutamate, ROS and glutathione levels in MECP2-KO astrocytes.

Astrocytes function to take up glutamate from synaptic space; excess glutamate can cause degeneration of neurons, excitotoxicity and seizures in various CNS diseases (Dong, Wang et al. 2009). Previous studies have reported high levels of excitatory neurotransmitter glutamate in the cerebrospinal fluid of patients with mutations in *MECP2* (Lappalainen and Riikonen 1996, Pan, Lane et al. 1999). Animal studies have shown contradicting results, with accelerated glutamate clearance in mutant astrocytes. MeCP2 has been shown to modulate glutamate clearance through regulation of various astroglia genes (Okabe, Takahashi et al. 2012) We corroborate the findings in humans as we observe significantly higher levels of extracellular glutamate in media conditioned from MeCP2-KO astrocytes when compared to control astrocytes (**Fig. 3b**). Inhibition of LINE-1 RT significantly decreases these levels whereas this rescue is not observed in the NVP condition **(Fig. 3b)**. Interestingly, one study reports that glutamate uptake by astrocytes is inhibited by a reactive oxygen species (ROS) intermediate (Piani, Frei et al. 1993). We analyzed the levels of ROS in our cultures and found a 5.5-fold increase in ROS levels coming from mutant astrocytes **(Fig. 3c).** Again, MECP2-KO astrocytes treated with LINE-1 RTi showed significantly lower levels of ROS. There was a reduction in ROS in the NVP treatment, but these were still significantly higher than the RTi treatment **(Fig. 3c).**

Glutathione is an antioxidant synthesized by glutathione synthetase and released by astrocytes in response to conditions of oxidative stress, inflammation or infection (Miller, Lawrence et al. 2009, Robinson, Lee et al. 2015). Glutathione pathways catalyze the reduction of ROS and so

we would expect to see elevated production of glutathione in mutant astrocytes. We found elevated levels of intracellular glutathione in MECP2-KO astrocytes, indicative of oxidative stress **(Fig. 3d)**. These levels are significantly reduced with RTi treatment. Treatment with NVP results in some reduction, but not to the same extent **(Fig. 3d)**. Taken together, these results suggest that derepression of LINE-1 elements, caused by mutations in *MECP2*, contribute to altered glutamate levels and an increase of oxidative stress in astrocytes. Additionally, these phenotypes can be rescued with chronic RTi treatment, possible leading to an improvement of the neural phenotype *in vitro.*

Rate of Ca^{2+} flux in in MECP2-KO neurons and astrocytes are improved with RTi treatments.

Early in neural development, spontaneous electrical activity leads to an increase in intracellular calcium levels important in regulating neuronal processes (Spitzer et al., 2004). Aberrant calcium signaling has been demonstrated in MeCP2 loss-of-function neurons and astrocytes (Marchetto, Carromeu et al. 2010, Dong, Liu et al. 2018). In order to investigate whether LINE-1 activation plays a role in abnormal calcium signaling, we measured the rate of spontaneous calcium flux using Rhod-4 dye and measuring fluorescence intensity at Ex/Em = 540/590 nm in a coculture of neurons and astrocytes. Images were acquired for 20 seconds (approximately 600 frames) per field. Region of interests (ROI) were selected manually by analyzing the cells waveform, a representative example of calcium tracing in neurons and astrocytes is depicted **(Fig 3e-f)**. We quantified the average number of calcium burst in 5 min and found a significant decrease in calcium event frequency in MECP2-KO astrocytes when compared to CTRL. Mutant astrocytes treated with RTi trend towards an increased rate of flux, but this did not reach significance. **(Fig 3h).** There is a significant improvement in the NVP treated conditions although total number of ROIs found per field was reduced in the UNT and NVP condition. Rate of calcium flux between

MECP2-KO and CTRL neurons were not significantly different, although we do observe a significant increase in rate of flux in both chronic RTi and NVP treatment **(Fig 3g).** Our data indicates an altered calcium activity associated with the MeCP2 deficiency, suggesting a potential imbalance in the neuronal networks.

DISCUSSION

Cellular models, such as the one represented here, can be used to study the altered physiology of various cell types derived from patients with neurological disorders. Neuroinflammation is a hallmark of many neurodegenerative disorders; abnormal activation of innate immune responses and subsequent secretion of neuroinflammatory markers have been shown to exacerbate disease pathologies. Mutations in *MECP2* and subsequent morphological and functional deficits observed in neurons and astrocytes has been extensively studied *in vivo* and *in vitro*. Patients with mutations in *MECP2* display subclinical inflammation profiles and dysregulation of chemokine and cytokine expression (Cortelazzo, De Felice et al. 2014, Cortelazzo, De Felice et al. 2017). Evidence supports immunological defects and immunodeficiency in patients, resulting from mis regulated internal inflammatory responses (van der Vaart, Svoboda et al. 2017). The driving mechanisms behind these phenotypes, be it genetic, epigenetic, or cellular influence, is not fully understood. Here we propose LINE-1 activation as a contributor to MeCP2 loss of function phenotypes.

Barbara McClintock laid the foundation for transposable element (TE) research with her discoveries in maize almost 80 years ago. The Human Genome Project then estimated that up to 45% of the genome is derived from TE sequences. Since then, research has focused on understanding how these elements become active and how they initiate and/or contribute to disease (Hancks and Kazazian 2016). Aberrant activation of LINE-1 retrotransposons have been implicated many diseased states, and accumulating evidence also reports LINE-1 intermediates as contributors to interferon- mediated inflammation. Endogenous retroelements have been linked as key effectors of inflammation in various autoimmune and neurodegenerative disorders, reviewed in (Saleh, Macia et al. 2019). When host mechanisms that work to repress LINE-1 fail, as seen in aging and cellular senescence, there is an accumulation of cytoplasmic LINE-1 DNA, resulting in

persistent inflammation (Thomas, Tejwani et al. 2017, De Cecco, Ito et al. 2019, Simon, Van Meter et al. 2019, Tharp, Malki et al. 2020).

In this thesis, we corroborate these findings. We report elevated LINE-1 ORF1 and ORF2 sequences in the extrachromosomal fractions of MECP2-KO neurons. We speculate that LINE- RT activity may be occurring preemptively outside of the nucleus, generating cDNA copies in the cytoplasm. Treatment with RTi successfully reduce the levels of LINE-1 cytoplasmic DNA. LINE-1 copies are likely accumulated due to the fact that MeCP2 is no longer repressing the transcription of the element. Previous research from our lab has shown improvements to MECP2-KO neuronal phenotypes with chronic RTi treatment (unpublished). We generated astrocytes with and without chronic RTi treatment in order to study the effects of these elements in a neuroinflammatory context. We report improvements in inflammatory gene expression signature of mutant astrocytes treated with RTis. Biological processes associated with the observed gene expression differences involve cytokine-cytokine receptor interactions, JAK/STAT signaling, cytoplasmic-DNA sensing (TMEM173), as well as interleukin and toll-like receptor signaling. Our evidence suggests LINE-1 retrotransposons as triggers for adaptive and innate immune responses in MECP2 loss-of-function astrocytes.

We followed our gene expression results with a variety of functional assays to investigate the connection between LINE-1 activation and astrocyte neurotoxicity and oxidative stress. Glutamate, a major excitatory neurotransmitter, is taken up by astrocytes to prevent prolonged exposure and neuronal excitotoxicity. Our results corroborate studies done in humans, which report elevated glutamate concentration in the CSF of patients with *MECP2* mutations. Mutant astrocytes cultures showed elevated extracellular glutamate concentrations, potentially due to disrupted clearance from mutant astrocytes. MeCP2 has been shown to modulate glutamate clearance through regulation of various astroglia genes (Okabe, Takahashi et al. 2012). RTi treatments rescue

glutamate concentrations to near control levels, likely due by preventing of activation of DNA-sensing pathways in the cell cytoplasm. Interestingly, due to the elevated levels of glutamate, we would expect an increase of calcium influx. However, the data matches observations made in (Marchetto, Carromeu et al. 2010). A possible explanation could be that our *in vitro* model mimics the early stages of brain development and this disturbance in calcium homeostasis could indicate a failure of astrocytic maturation in the cells.

In addition, previous studies report glutamate uptake by astrocytes is inhibited by a reactive oxygen species (ROS) intermediate (Piani, Frei et al. 1993). Strikingly, we detected 5.5-fold increase in ROS levels from mutant astrocyte cultures. This could potentially explain deficits in glutamate uptake. Both ROS and glutathione levels were rescued with RTi treatment, indicating LINE-1 activity as a contributor to oxidative stress.

Taken together, we uncovered for the first time an accumulation of cytoplasmic LINE-1 copies in a model for Rett Syndrome and found that the mis regulation of these elements promotes inflammatory and toxic effects in human astrocytes. In addition, we found that by treating the affected cells with FDA-approved RT inhibitors, we are able to rescue the observed phenotype, suggesting the finding of a novel target for future effective treatments. To further confirm the results found in this study, targeted LINE-1 inhibition through multiple modalities should be performed in future experiments. Apart from RTi treatment, which provides an effective potential therapy, astrocyte phenotypes in MECP-KO cells should be explored by targeting the LINE-1 transcript using short hairpin or short interfering RNA tools (shRNA/siRNA), as previously described (Thomas, Tejwani et al. 2017). In sum, this system provides a platform to further investigate the relationship between LINE-1 activity as a contributor to neurodevelopmental disorders, cytosolic DNA response and neuroinflammation.

FIGURES

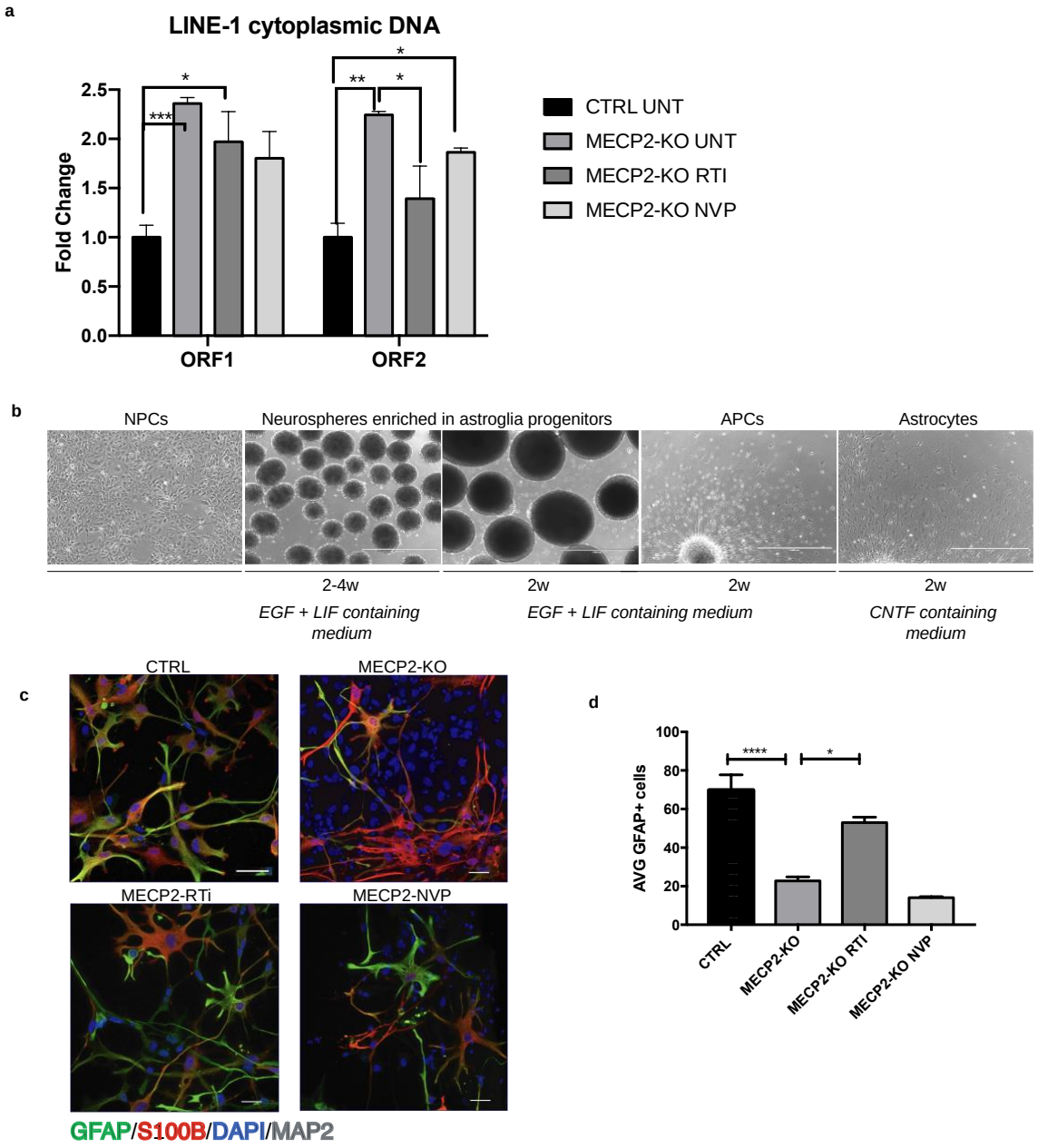

Figure 1. RTi treatment decreases cytoplasmic LINE-1 DNA in neurons and increases the number of GFAP expressing cells in astrocytes.

a. qPCR of cytoplasmic extrachromosomal DNA extracted from CTRL and MECP2-KO neurons with or without chronic RTi treatment. Primers against ORF1 and ORF2 sequences were used. Error bars represent s.e.m. Expression is normalized to CTRL equaling one. **b.** iPSC-derived astrocytes. NPCs were cultured in suspension in media containing EGF and LIF for 2-4w. Spheres were expanded in medium containing EGF and FGF for 2w. Monolayer culture of astrocyte progenitors (APC) were obtained by plating the spheres and allowing progenitors to grow radially. Astrocytes were generated after 14 d of CNTF containing medium. **c.** Differentiation with CNTF generated astrocytes that were GFAP+, S100B+. Cultures were negative for neuronal marker MAP2. Scale bar, 50 µm **d**. Quantification of number of GFAP+ astrocytes from MECP2-KO and CTRL cell line with and without RTi and NVP treatment. *p<0.05,***p< 0.001,****p< 0.0001, One-way ANOVA and Tukey's multiple comparisons test.

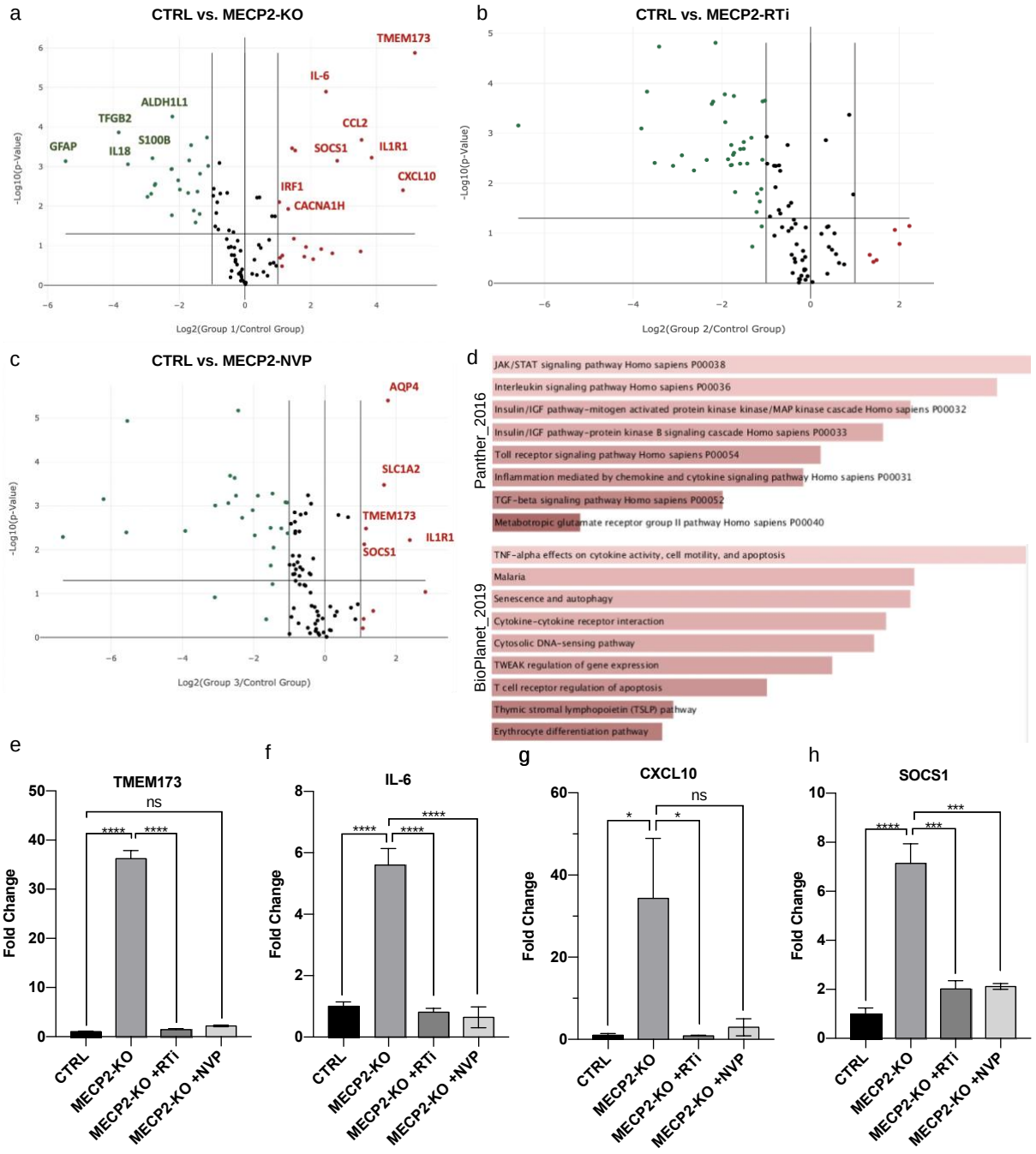

Figure 2. Genes involved in cytokine expression and innate immunity are upregulated in mutant astrocytes and decreased with RTi and NVP treatment.

a-c Volcano plot of statistical significance (p-value, -log10) against fold-change (FC, $\log_2$) differential gene expression between CTRL and MECP2-KO, CTRL and MECP2-RTi, and CTRL and NVP treated astrocytes. Minimum 2-fold change. Horizontal bar represents statistical significance p value <0.05. **d.** Pathway analysis with differentially expressed genes between CTRL and MECP2-KO. The length of the bar represents the significance of that specific gene-set or pathway. In addition, the brighter the color, the more significant that term is. **e-h**. Bar graph quantification of upregulated genes TMEM173, Il-6, CXCL10, SOCS1. n=3. error bars represent ± s.e.m. *p<0.05,***p< 0.001,****p< 0.0001, n.s not significant. One-way ANOVA and Tukey's multiple comparisons test.

Figure 3. Chronic treatment with RTis improves measures of astrocyte neurotoxicity, oxidative stress, and Ca^{2+} event frequency.
a. CTRL and MECP2-KO astrocytes were cultured for 14 days with CNTF and conditioned media was collected 48h after last media change. ELISA detecting levels of proinflammatory cytokine IL-6 secreted from CTRL and MECP2-KO astrocytes with and without RTi treatment. **b.** Extracellular glutamate levels of astrocytes treated with RTi represented with fold increase. **c.** Fold increase for levels of reactive oxygen species (ROS) in astrocyte cultures. **d.** Fold-change differences in levels of intracellular glutathione from CTRL and MECP2-KO astrocytes with and without RTi treatment. Data are shown as mean ± s.e.m.. *p<0.05, ***p< 0.001,****p< 0.0001, n.s not significant. One-way ANOVA and Tukey's multiple comparisons test. **e**. Classification of neuron and astrocyte traces with Netcal program. **f.** Corresponding waveforms of Ca^{2+} fluorescence intensity in neurons and astrocytes. **g-h.** Calcium flux events in neuron and astrocytes from CTRL and MECP2-KO backgrounds. MECP2-KO cells were treated with RTi and NVP. Fluorescence intensity at Ex/Em = 540/590 nm. Images were acquired for 20 seconds (approximately 600 frames) per field. Data is number of bursts/ 5min.

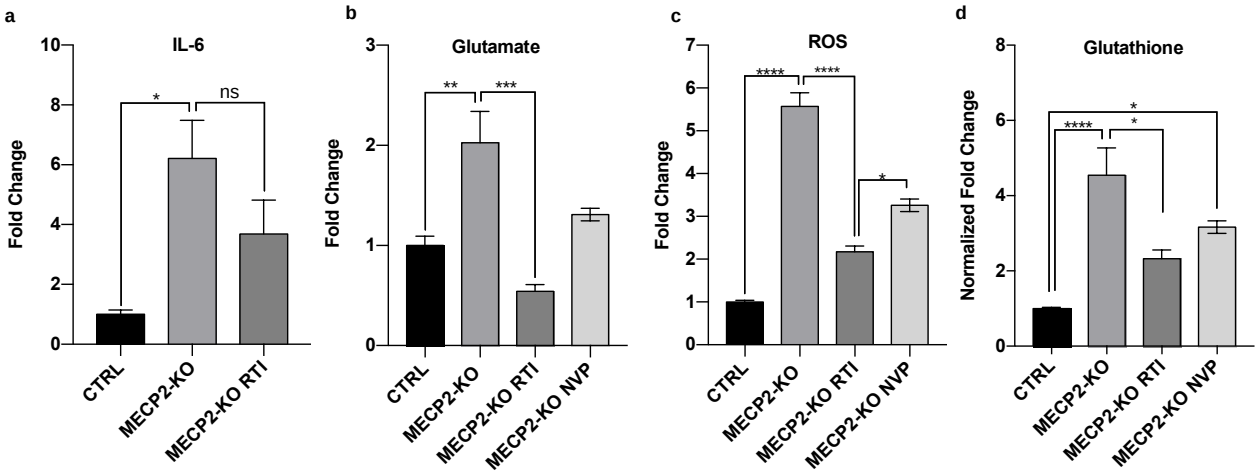
a
IL-6
Fold Change
*
ns
CTRL
MECP2-KO
MECP2-KO RTI
b
Glutamate
Fold Change
**
***
CTRL
MECP2-KO
MECP2-KO RTI
MECP2-KO NVP
c
ROS
Fold Change
****
****
*
CTRL
MECP2-KO
MECP2-KO RTI
MECP2-KO NVP
d
Glutathione
Normalized Fold Change
*
****
*
CTRL
MECP2-KO
MECP2-KO RTI
MECP2-KO NVP

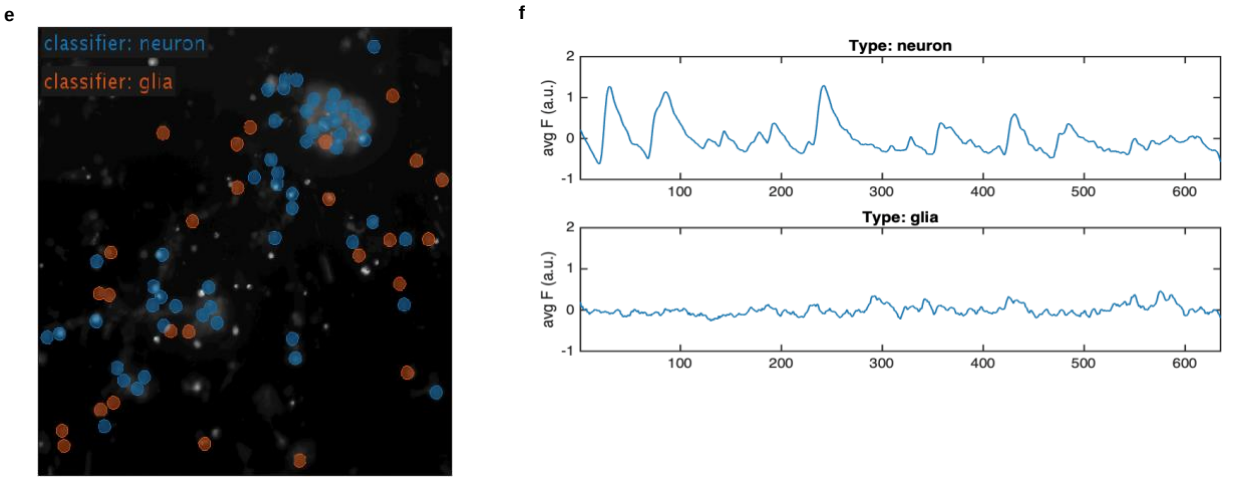
e
classifier: neuron
classifier: glia
f
Type: neuron
avg F (a.u.)
Type: glia
avg F (a.u.)

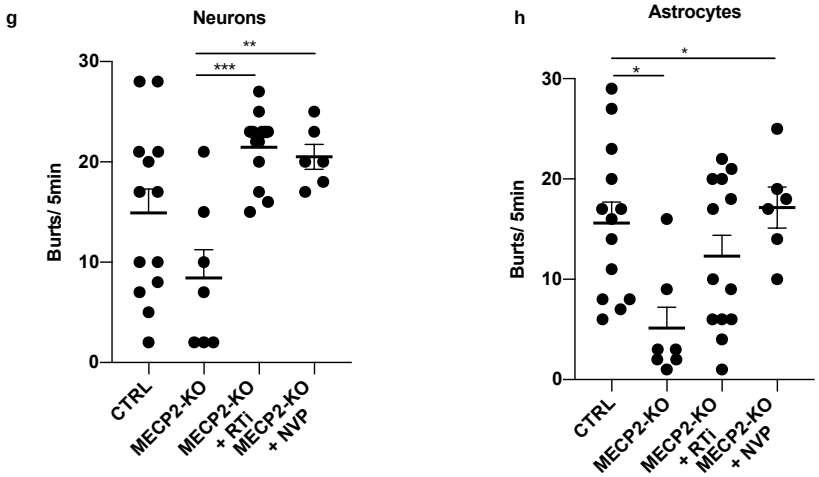
g
Neurons
Burts/ 5min
**
***
CTRL
MECP2-KO
MECP2-KO + RTi
MECP2-KO + NVP
h
Astrocytes
Burts/ 5min
*
*
CTRL
MECP2-KO
MECP2-KO + RTi
MECP2-KO + NVP

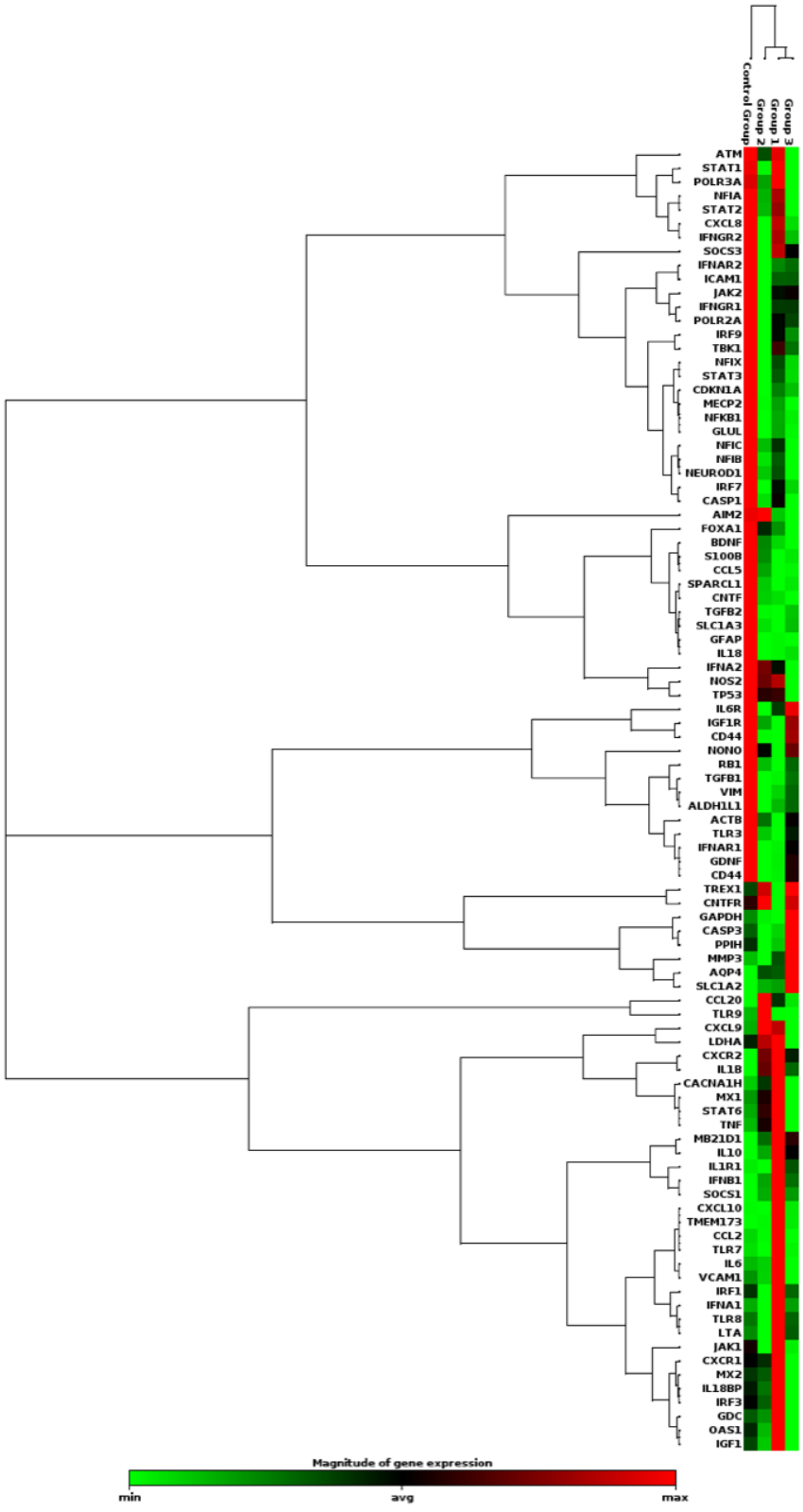

Figure S1. Clustergram analysis, heat map of gene expression data. Groups 1, 2, and 3, represent MECP2-KO, MECP2 RTi, and MECP2-NVP, respectively. Note that MECP2-KO RTi group clusters closer to the control cells. Green and red color represents dowregulated and upregulated genes, respectively.

.

Table 1. PCR array gene list

Position	Unigene	Refseq	Symbol	Description
1	Hs.200716	NM_004992	MECP2	Methyl CpG binding protein 2 (Rett syndrome)
2	Hs.514227	NM_002055	GFAP	Glial fibrillary acidic protein
3	Hs.422181	NM_006272	S100B	S100 calcium binding protein B
4	Hs.455493	NM_003380	VIM	Vimentin
5	Hs.315369	NM_001650	AQP4	Aquaporin 4
6	Hs.62886	NM_004684	SPARCL1	SPARC-like 1 (hevin)
7	Hs.654458	NM_000600	IL6	Interleukin 6 (interferon, beta 2)
8	Hs.135087	NM_000565	IL6R	Interleukin 6 receptor
9	Hs.624	NM_000584	CXCL8	Interleukin 8
10	Hs.194778	NM_000634	CXCR1	Chemokine (C-X-C motif) receptor 1
11	Hs.846	NM_001557	CXCR2	Chemokine (C-X-C motif) receptor 2
12	Hs.83077	NM_001562	IL18	Interleukin 18 (interferon-gamma-inducing factor)
13	Hs.740757	NM_005595	NFIA	Nuclear factor I/A
14	Hs.644095	NM_005596	NFIB	Nuclear factor I/B
15	Hs.170131	NM_005597	NFIC	Nuclear factor I/C (CCAAT-binding transcription factor)
16	Hs.257970	NM_002501	NFIX	Nuclear factor I/X (CCAAT-binding transcription factor)
17	Hs.207538	NM_002227	JAK1	Janus kinase 1
18	Hs.656213	NM_004972	JAK2	Janus kinase 2
19	Hs.591967	NM_00103965	IL18BP	Interleukin 18 binding protein
20	Hs.529400	NM_000629	IFNAR1	Interferon (alpha, beta and omega) receptor 1
21	Hs.37026	NM_024013	IFNA1	Interferon, alpha 1
22	Hs.708195	NM_000874	IFNAR2	Interferon (alpha, beta and omega) receptor 2
23	Hs.93177	NM_002176	IFNB1	Interferon, beta 1, fibroblast
24	Hs.520414	NM_000416	IFNGR1	Interferon gamma receptor 1
25	Hs.642990	NM_007315	STAT1	Signal transducer and activator of transcription 1, 91kDa
26	Hs.530595	NM_005419	STAT2	Signal transducer and activator of transcription 2, 113kDa
27	Hs.524518	NM_003153	STAT6	Signal transducer and activator of transcription 6, interleukin-4 induced
28	Hs.241570	NM_000594	TNF	Tumor necrosis factor
29	Hs.658405	NM_138441	MB21D1	Mab-21 domain containing 1
30	Hs.126256	NM_000576	IL1B	Interleukin 1, beta
31	Hs.634632	NM_005534	IFNGR2	Interferon gamma receptor 2 (interferon gamma transducer 1)
32	Hs.248114	NM_000514	GDNF	Glial cell derived neurotrophic factor
33	Hs.524760	NM_002534	OAS1	2'-5'-oligoadenylate synthetase 1, 40/46kDa
34	Hs.517307	NM_002462	MX1	Myxovirus (influenza virus) resistance 1, interferon-inducible protein p78 (mouse)
35	Hs.436061	NM_002198	IRF1	Interferon regulatory factor 1
36	Hs.1706	NM_006084	IRF9	Interferon regulatory factor 9
37	Hs.618430	NM_003998	NFKB1	Nuclear factor of kappa light polypeptide gene enhancer in B-cells 1
38	Hs.166120	NM_001572	IRF7	Interferon regulatory factor 7
39	Hs.289052	NM_001571	IRF3	Interferon regulatory factor 3
40	Hs.505874	NM_013254	TBK1	TANK-binding kinase 1
41	Hs.303649	NM_002982	CCL2	Chemokine (C-C motif) ligand 2
42	Hs.75498	NM_004591	CCL20	Chemokine (C-C motif) ligand 20
43	Hs.77367	NM_002416	CXCL9	Chemokine (C-X-C motif) ligand 9
44	Hs.375129	NM_002422	MMP3	Matrix metallopeptidase 3 (stromelysin 1, progelatinase)
45	Hs.707026	NM_016381	TREX1	Three prime repair exonucl ease 1
46	Hs.163484	NM_004496	FOXA1	Forkhead box A1
47	Hs.408528	NM_000321	RB1	Retinoblastoma 1
48	Hs.370771	NM_000389	CDKN1A	Cyclin-dependent kinase inhibitor 1A (p21, Cip1)

49	Hs.463059	NM_003150	STAT3	Signal transducer and activator of transcription 3 (acute-phase response factor)
50	Hs.211575	NM_00605		
51	Hs.926	NM_002463	MX2	Myxovirus (influenza virus) resistance 2 (mouse)
52	Hs.50640	NM_003745	SOCS1	Suppressor of cytokine signaling 1
53	Hs.527973	NM_003955	SOCS3	Suppressor of cytokine signaling 3
54	Hs.160562	NM_000618	IGF1	Insulin-like growth factor 1 (somatomedin C)
55	Hs.643447	NM_000201	ICAM1	Intercellular adhesion molecule 1
56	Hs.459642	NM_021098	CACNA1H	Calcium channel, voltage-dependent, T type, alpha 1H subunit
57	Hs.141125	NM_004346	CASP3	Caspase 3, apoptosis-related cysteine peptidase
58	Hs.733411	NM_004833	AIM2	Absent in melanoma 2
59	Hs.87968	NM_017442	TLR9	Toll-like receptor 9
60	Hs.632586	NM_001565	CXCL10	Chemokine (C-X-C motif) ligand 10
61	Hs.643120	NM_000875	IGF1R	Insulin-like growth factor 1 receptor
62	Hs.645227	NM_000660	TGFB1	Transforming growth factor, beta 1
63	Hs.133379	NM_003238	TGFB2	Transforming growth factor, beta 2
64	Hs.524920	NM_000614	CNTF	Ciliary neurotrophic factor
65	Hs.129966	NM_001842	CNTFR	Ciliary neurotrophic factor receptor
66	Hs.481918	NM_004172	SLC1A3	Solute carrier family 1 (glial high affinity glutamate transporter), member 3
67	Hs.436896	NM_007055	POLR3A	Polymerase (RNA) III (DNA directed) polypeptide A, 155kDa
68	Hs.270017	NM_000937	POLR2A	Polymerase (RNA) II (DNA directed) polypeptide A, 220kDa
69	Hs.657724	NM_003265	TLR3	Toll-like receptor 3
70	Hs.659215	NM_016562	TLR7	Toll-like receptor 7
71	Hs.660543	NM_138636	TLR8	Toll-like receptor 8
72	Hs.514821	NM_002985	CCL5	Chemokine (C-C motif) ligand 5
73	Hs.502338	NM_004171	SLC1A2	Solute carrier family 1 (glial high affinity glutamate transporter), member 2
74	Hs.132016	NM_002065	GLUL	Glutamate-ammonia ligase
75	Hs.434435	NM_012190	ALDH1L1	Aldehyde dehydrogenase 1 family, member L1
76	Hs.502328	NM_000610	CD44	CD44 molecule (Indian blood group)
77	Hs.379754	NM_198282	TMEM173	Transmembrane protein 173
78	Hs.2490	NM_033292	CASP1	Caspase 1, apoptosis-related cysteine peptidase (interleukin 1, beta, convertase)
79	Hs.193717	NM_000572	IL10	Interleukin 10
80	Hs.709191	NM_000625	NOS2	Nitric oxide synthase 2, inducible
81	Hs.36	NM_000595	LTA	Lymphotoxin alpha (TNF superfamily, member 1)
82	Hs.701982	NM_000877	IL1R1	Interleukin 1 receptor, type I
83	Hs.502182	NM_001709	BDNF	Brain-derived neurotrophic factor
84	Hs.574626	NM_002500	NEUROD1	Neurogenic differentiation 1
85	Hs.367437	NM_000051	ATM	Ataxia telangiectasia mutated
86	Hs.437460	NM_000546	TP53	Tumor protein p53
87	Hs.502328	NM_000610	CD44	CD44 molecule (Indian blood group)
88	Hs.109225	NM_001078	VCAM1	Vascular cell adhesion molecule 1
89	Hs.729213	NM_006347	PPIH	Peptidylprolyl isomerase H (cyclophilin H)
90	Hs.592355	NM_002046	GAPDH	Glyceraldehyde-3-phosphate dehydrogenase
91	Hs.533282	NM_007363	NONO	Non-POU domain containing, octamer-binding

92	Hs.2795	NM_005566	LDHA	Lactate dehydrogenase A
93	Hs.520640	NM_001101	ACTB	Actin, beta
94	N/A	SA_00104	RTC	Reverse Transcription Control

REFERENCES

Aber, K. M., P. Nori, S. M. MacDonald, G. Bibat, M. H. Jarrar and W. E. Kaufmann (2003). "Methyl-CpG-binding protein 2 is localized in the postsynaptic compartment: an immunochemical study of subcellular fractions." Neuroscience **116**(1): 77-80.

Ahmed, R. (2007). "Clinical profile of five patients with Rett syndrome and literature review." Oman Med J **22**(3): 64-66.

Arad, U. (1998). "Modified Hirt procedure for rapid purification of extrachromosomal DNA from mammalian cells." Biotechniques **24**(5): 760-762.

Armstrong, D., J. K. Dunn, B. Antalffy and R. Trivedi (1995). "Selective dendritic alterations in the cortex of Rett syndrome." J Neuropathol Exp Neurol **54**(2): 195-201.

Baillie, J. K., M. W. Barnett, K. R. Upton, D. J. Gerhardt, T. A. Richmond, F. De Sapio, P. M. Brennan, P. Rizzu, S. Smith, M. Fell, R. T. Talbot, S. Gustincich, T. C. Freeman, J. S. Mattick, D. A. Hume, P. Heutink, P. Carninci, J. A. Jeddeloh and G. J. Faulkner (2011). "Somatic retrotransposition alters the genetic landscape of the human brain." Nature **479**(7374): 534-537.

Belichenko, P. V., E. E. Wright, N. P. Belichenko, E. Masliah, H. H. Li, W. C. Mobley and U. Francke (2009). "Widespread changes in dendritic and axonal morphology in Mecp2-mutant mouse models of Rett syndrome: evidence for disruption of neuronal networks." J Comp Neurol **514**(3): 240-258.

Boissinot, S., A. Entezam and A. V. Furano (2001). "Selection against deleterious LINE-1-containing loci in the human lineage." Mol Biol Evol **18**(6): 926-935.

Brouha, B., J. Schustak, R. M. Badge, S. Lutz-Prigge, A. H. Farley, J. V. Moran and H. H. Kazazian, Jr. (2003). "Hot L1s account for the bulk of retrotransposition in the human population." Proc Natl Acad Sci U S A **100**(9): 5280-5285.

Carter, J. C., D. C. Lanham, D. Pham, G. Bibat, S. Naidu and W. E. Kaufmann (2008). "Selective cerebral volume reduction in Rett syndrome: a multiple-approach MR imaging study." AJNR Am J Neuroradiol **29**(3): 436-441.

Chahrour, M., S. Y. Jung, C. Shaw, X. Zhou, S. T. Wong, J. Qin and H. Y. Zoghbi (2008).

"MeCP2, a key contributor to neurological disease, activates and represses transcription." Science **320**(5880): 1224-1229.

Chen, J. M., P. D. Stenson, D. N. Cooper and C. Ferec (2005). "A systematic analysis of LINE-1 endonuclease-dependent retrotranspositional events causing human genetic disease." Hum Genet **117**(5): 411-427.

Chuong, E. B., N. C. Elde and C. Feschotte (2016). "Regulatory evolution of innate immunity through co-option of endogenous retroviruses." Science **351**(6277): 1083-1087.

Colombo, E. and C. Farina (2016). "Astrocytes: Key Regulators of Neuroinflammation." Trends Immunol **37**(9): 608-620.

Cordaux, R. and M. A. Batzer (2009). "The impact of retrotransposons on human genome evolution." Nat Rev Genet **10**(10): 691-703.

Cortelazzo, A., C. De Felice, B. De Filippis, L. Ricceri, G. Laviola, S. Leoncini, C. Signorini, M. Pescaglini, R. Guerranti, A. M. Timperio, L. Zolla, L. Ciccoli and J. Hayek (2017). "Persistent Unresolved Inflammation in the Mecp2-308 Female Mutated Mouse Model of Rett Syndrome." Mediators Inflamm **2017**: 9467819.

Cortelazzo, A., C. De Felice, R. Guerranti, C. Signorini, S. Leoncini, A. Pecorelli, G. Zollo, C. Landi, G. Valacchi, L. Ciccoli, L. Bini and J. Hayek (2014). "Subclinical inflammatory status in Rett syndrome." Mediators Inflamm **2014**: 480980.

Cost, G. J. and J. D. Boeke (1998). "Targeting of human retrotransposon integration is directed by the specificity of the L1 endonuclease for regions of unusual DNA structure." Biochemistry **37**(51): 18081-18093.

Coufal, N. G., J. L. Garcia-Perez, G. E. Peng, G. W. Yeo, Y. Mu, M. T. Lovci, M. Morell, K. S. O'Shea, J. V. Moran and F. H. Gage (2009). "L1 retrotransposition in human neural progenitor cells." Nature **460**(7259): 1127-1131.

Crow, M. K. (2010). "Long interspersed nuclear elements (LINE-1): potential triggers of systemic autoimmune disease." Autoimmunity **43**(1): 7-16.

Crow, Y. J. and J. Rehwinkel (2009). "Aicardi-Goutieres syndrome and related phenotypes: linking nucleic acid metabolism with autoimmunity." Hum Mol Genet **18**(R2): R130-136.

Dai, L., Q. Huang and J. D. Boeke (2011). "Effect of reverse transcriptase inhibitors on LINE-1 and Ty1 reverse transcriptase activities and on LINE-1 retrotransposition." BMC Biochem **12**: 18.

De Cecco, M., T. Ito, A. P. Petrashen, A. E. Elias, N. J. Skvir, S. W. Criscione, A. Caligiana, G. Brocculi, E. M. Adney, J. D. Boeke, O. Le, C. Beausejour, J. Ambati, K. Ambati, M. Simon, A. Seluanov, V. Gorbunova, P. E. Slagboom, S. L. Helfand, N. Neretti and J. M. Sedivy (2019). "L1 drives IFN in senescent cells and promotes age-associated inflammation." Nature **566**(7742): 73-78.

de Souza, J. S., C. Carromeu, L. B. Torres, B. H. Araujo, F. R. Cugola, R. M. Maciel, A. R. Muotri and G. Giannocco (2017). "IGF1 neuronal response in the absence of MECP2 is dependent on TRalpha 3." Hum Mol Genet **26**(2): 270-281.

Delepine, C., H. Meziane, J. Nectoux, M. Opitz, A. B. Smith, C. Ballatore, Y. Saillour, A. Bennaceur-Griscelli, Q. Chang, E. C. Williams, M. Dahan, A. Duboin, P. Billuart, Y. Herault and T. Bienvenu (2016). "Altered microtubule dynamics and vesicular transport in mouse and human MeCP2-deficient astrocytes." Hum Mol Genet **25**(1): 146-157.

Deniz, O., J. M. Frost and M. R. Branco (2019). "Author Correction: Regulation of transposable elements by DNA modifications." Nat Rev Genet.

Dewannieux, M., C. Esnault and T. Heidmann (2003). "LINE-mediated retrotransposition of marked Alu sequences." Nat Genet **35**(1): 41-48.

Dong, Q., Q. Liu, R. Li, A. Wang, Q. Bu, K. H. Wang and Q. Chang (2018). "Mechanism and consequence of abnormal calcium homeostasis in Rett syndrome astrocytes." Elife **7**.

Dong, X. X., Y. Wang and Z. H. Qin (2009). "Molecular mechanisms of excitotoxicity and their relevance to pathogenesis of neurodegenerative diseases." Acta Pharmacol Sin **30**(4): 379-387.

Doucet, A. J., A. E. Hulme, E. Sahinovic, D. A. Kulpa, J. B. Moldovan, H. C. Kopera, J. N. Athanikar, M. Hasnaoui, A. Bucheton, J. V. Moran and N. Gilbert (2010). "Characterization of LINE-1 ribonucleoprotein particles." PLoS Genet **6**(10).

Elbarbary, R. A., B. A. Lucas and L. E. Maquat (2016). "Retrotransposons as regulators of gene expression." Science **351**(6274): aac7247.

Estecio, M. R., J. Gallegos, M. Dekmezian, Y. Lu, S. Liang and J. P. Issa (2012). "SINE

retrotransposons cause epigenetic reprogramming of adjacent gene promoters." Mol Cancer Res **10**(10): 1332-1342.

Ezeonwuka, C. D. and M. Rastegar (2014). "MeCP2-Related Diseases and Animal Models." Diseases **2**(1): 45-70.

Gilbert, N., S. Lutz-Prigge and J. V. Moran (2002). "Genomic deletions created upon LINE-1 retrotransposition." Cell **110**(3): 315-325.

Goodier, J. L. and H. H. Kazazian, Jr. (2008). "Retrotransposons revisited: the restraint and rehabilitation of parasites." Cell **135**(1): 23-35.

Goodier, J. L., L. Zhang, M. R. Vetter and H. H. Kazazian, Jr. (2007). "LINE-1 ORF1 protein localizes in stress granules with other RNA-binding proteins, including components of RNA interference RNA-induced silencing complex." Mol Cell Biol **27**(18): 6469-6483.

Hancks, D. C. and H. H. Kazazian, Jr. (2016). "Roles for retrotransposon insertions in human disease." Mob DNA **7**: 9.

Hatanaka, Y., K. Inoue, M. Oikawa, S. Kamimura, N. Ogonuki, E. N. Kodama, Y. Ohkawa, Y. Tsukada and A. Ogura (2015). "Histone chaperone CAF-1 mediates repressive histone modifications to protect preimplantation mouse embryos from endogenous retrotransposons." Proc Natl Acad Sci U S A **112**(47): 14641-14646.

Hite, K. C., V. H. Adams and J. C. Hansen (2009). "Recent advances in MeCP2 structure and function." Biochem Cell Biol **87**(1): 219-227.

Huang, C. R., K. H. Burns and J. D. Boeke (2012). "Active transposition in genomes." Annu Rev Genet **46**: 651-675.

Jurka, J. (1997). "Sequence patterns indicate an enzymatic involvement in integration of mammalian retroposons." Proc Natl Acad Sci U S A **94**(5): 1872-1877.

Kano, H., I. Godoy, C. Courtney, M. R. Vetter, G. L. Gerton, E. M. Ostertag and H. H. Kazazian, Jr. (2009). "L1 retrotransposition occurs mainly in embryogenesis and creates somatic mosaicism." Genes Dev **23**(11): 1303-1312.

Kery, R., A. P. F. Chen and G. W. Kirschen (2020). "Genetic targeting of astrocytes to combat

neurodegenerative disease." Neural Regen Res **15**(2): 199-211.

Kulpa, D. A. and J. V. Moran (2005). "Ribonucleoprotein particle formation is necessary but not sufficient for LINE-1 retrotransposition." Hum Mol Genet **14**(21): 3237-3248.

Lander, E. S., L. M. Linton, B. Birren, C. Nusbaum, M. C. Zody, J. Baldwin, K. Devon, K. Dewar, M. Doyle, W. FitzHugh, R. Funke, D. Gage, K. Harris, A. Heaford, J. Howland, L. Kann, J. Lehoczky, R. LeVine, P. McEwan, K. McKernan, J. Meldrim, J. P. Mesirov, C. Miranda, W. Morris, J. Naylor, C. Raymond, M. Rosetti, R. Santos, A. Sheridan, C. Sougnez, Y. Stange-Thomann, N. Stojanovic, A. Subramanian, D. Wyman, J. Rogers, J. Sulston, R. Ainscough, S. Beck, D. Bentley, J. Burton, C. Clee, N. Carter, A. Coulson, R. Deadman, P. Deloukas, A. Dunham, I. Dunham, R. Durbin, L. French, D. Grafham, S. Gregory, T. Hubbard, S. Humphray, A. Hunt, M. Jones, C. Lloyd, A. McMurray, L. Matthews, S. Mercer, S. Milne, J. C. Mullikin, A. Mungall, R. Plumb, M. Ross, R. Shownkeen, S. Sims, R. H. Waterston, R. K. Wilson, L. W. Hillier, J. D. McPherson, M. A. Marra, E. R. Mardis, L. A. Fulton, A. T. Chinwalla, K. H. Pepin, W. R. Gish, S. L. Chissoe, M. C. Wendl, K. D. Delehaunty, T. L. Miner, A. Delehaunty, J. B. Kramer, L. L. Cook, R. S. Fulton, D. L. Johnson, P. J. Minx, S. W. Clifton, T. Hawkins, E. Branscomb, P. Predki, P. Richardson, S. Wenning, T. Slezak, N. Doggett, J. F. Cheng, A. Olsen, S. Lucas, C. Elkin, E. Uberbacher, M. Frazier, R. A. Gibbs, D. M. Muzny, S. E. Scherer, J. B. Bouck, E. J. Sodergren, K. C. Worley, C. M. Rives, J. H. Gorrell, M. L. Metzker, S. L. Naylor, R. S. Kucherlapati, D. L. Nelson, G. M. Weinstock, Y. Sakaki, A. Fujiyama, M. Hattori, T. Yada, A. Toyoda, T. Itoh, C. Kawagoe, H. Watanabe, Y. Totoki, T. Taylor, J. Weissenbach, R. Heilig, W. Saurin, F. Artiguenave, P. Brottier, T. Bruls, E. Pelletier, C. Robert, P. Wincker, D. R. Smith, L. Doucette-Stamm, M. Rubenfield, K. Weinstock, H. M. Lee, J. Dubois, A. Rosenthal, M. Platzer, G. Nyakatura, S. Taudien, A. Rump, H. Yang, J. Yu, J. Wang, G. Huang, J. Gu, L. Hood, L. Rowen, A. Madan, S. Qin, R. W. Davis, N. A. Federspiel, A. P. Abola, M. J. Proctor, R. M. Myers, J. Schmutz, M. Dickson, J. Grimwood, D. R. Cox, M. V. Olson, R. Kaul, C. Raymond, N. Shimizu, K. Kawasaki, S. Minoshima, G. A. Evans, M. Athanasiou, R. Schultz, B. A. Roe, F. Chen, H. Pan, J. Ramser, H. Lehrach, R. Reinhardt, W. R. McCombie, M. de la Bastide, N. Dedhia, H. Blocker, K. Hornischer, G. Nordsiek, R. Agarwala, L. Aravind, J. A. Bailey, A. Bateman, S. Batzoglou, E. Birney, P. Bork, D. G. Brown, C. B. Burge, L. Cerutti, H. C. Chen, D. Church, M. Clamp, R. R. Copley, T. Doerks, S. R. Eddy, E. E. Eichler, T. S. Furey, J. Galagan, J. G. Gilbert, C. Harmon, Y. Hayashizaki, D. Haussler, H. Hermjakob, K. Hokamp, W. Jang, L. S. Johnson, T. A. Jones, S. Kasif, A. Kaspryzk, S. Kennedy, W. J. Kent, P. Kitts, E. V. Koonin, I. Korf, D. Kulp, D. Lancet, T. M. Lowe, A. McLysaght, T. Mikkelsen, J. V. Moran, N. Mulder, V. J. Pollara, C. P. Ponting, G. Schuler, J. Schultz, G. Slater, A. F. Smit, E. Stupka, J. Szustakowki, D. Thierry-Mieg, J. Thierry-Mieg, L. Wagner, J. Wallis, R. Wheeler, A. Williams, Y. I. Wolf, K. H. Wolfe, S. P. Yang, R. F. Yeh, F. Collins, M. S. Guyer, J. Peterson, A. Felsenfeld, K. A. Wetterstrand, A. Patrinos, M. J. Morgan, P. de Jong, J. J. Catanese, K. Osoegawa, H. Shizuya, S. Choi, Y. J. Chen, J. Szustakowki and C. International Human Genome Sequencing (2001). "Initial sequencing and analysis of the human genome." Nature **409**(6822): 860-921.

Lappalainen, R. and R. S. Riikonen (1996). "High levels of cerebrospinal fluid glutamate in Rett

syndrome." Pediatr Neurol **15**(3): 213-216.

Lavie, L., E. Maldener, B. Brouha, E. U. Meese and J. Mayer (2004). "The human L1 promoter: variable transcription initiation sites and a major impact of upstream flanking sequence on promoter activity." Genome Res **14**(11): 2253-2260.

Lioy, D. T., S. K. Garg, C. E. Monaghan, J. Raber, K. D. Foust, B. K. Kaspar, P. G. Hirrlinger, F. Kirchhoff, J. M. Bissonnette, N. Ballas and G. Mandel (2011). "A role for glia in the progression of Rett's syndrome." Nature **475**(7357): 497-500.

Macia, A., E. Blanco-Jimenez and J. L. Garcia-Perez (2015). "Retrotransposons in pluripotent cells: Impact and new roles in cellular plasticity." Biochim Biophys Acta **1849**(4): 417-426.

Macia, A., M. Munoz-Lopez, J. L. Cortes, R. K. Hastings, S. Morell, G. Lucena-Aguilar, J. A. Marchal, R. M. Badge and J. L. Garcia-Perez (2011). "Epigenetic control of retrotransposon expression in human embryonic stem cells." Mol Cell Biol **31**(2): 300-316.

Maezawa, I., S. Swanberg, D. Harvey, J. M. LaSalle and L. W. Jin (2009). "Rett syndrome astrocytes are abnormal and spread MeCP2 deficiency through gap junctions." J Neurosci **29**(16): 5051-5061.

Maragakis, N. J. and J. D. Rothstein (2006). "Mechanisms of Disease: astrocytes in neurodegenerative disease." Nat Clin Pract Neurol **2**(12): 679-689.

Marchetto, M. C., C. Carromeu, A. Acab, D. Yu, G. W. Yeo, Y. Mu, G. Chen, F. H. Gage and A. R. Muotri (2010). "A model for neural development and treatment of Rett syndrome using human induced pluripotent stem cells." Cell **143**(4): 527-539.

Martin, S. L. and F. D. Bushman (2001). "Nucleic acid chaperone activity of the ORF1 protein from the mouse LINE-1 retrotransposon." Mol Cell Biol **21**(2): 467-475.

Martin, S. L., M. Cruceanu, D. Branciforte, P. Wai-Lun Li, S. C. Kwok, R. S. Hodges and M. C. Williams (2005). "LINE-1 retrotransposition requires the nucleic acid chaperone activity of the ORF1 protein." J Mol Biol **348**(3): 549-561.

Martinez de Paz, A. and J. Ausio (2017). "MeCP2, A Modulator of Neuronal Chromatin Organization Involved in Rett Syndrome." Adv Exp Med Biol **978**: 3-21.

Mathias, S. L., A. F. Scott, H. H. Kazazian, Jr., J. D. Boeke and A. Gabriel (1991). "Reverse transcriptase encoded by a human transposable element." Science **254**(5039): 1808-1810.

Miller, V. M., D. A. Lawrence, T. K. Mondal and R. F. Seegal (2009). "Reduced glutathione is highly expressed in white matter and neurons in the unperturbed mouse brain--implications for oxidative stress associated with neurodegeneration." Brain Res **1276**: 22-30.

Monot, C., M. Kuciak, S. Viollet, A. A. Mir, C. Gabus, J. L. Darlix and G. Cristofari (2013). "The specificity and flexibility of l1 reverse transcription priming at imperfect T-tracts." PLoS Genet **9**(5): e1003499.

Moran, J. V., S. E. Holmes, T. P. Naas, R. J. DeBerardinis, J. D. Boeke and H. H. Kazazian, Jr. (1996). "High frequency retrotransposition in cultured mammalian cells." Cell **87**(5): 917-927.

Muotri, A. R., V. T. Chu, M. C. Marchetto, W. Deng, J. V. Moran and F. H. Gage (2005). "Somatic mosaicism in neuronal precursor cells mediated by L1 retrotransposition." Nature **435**(7044): 903-910.

Muotri, A. R., M. C. Marchetto, N. G. Coufal, R. Oefner, G. Yeo, K. Nakashima and F. H. Gage (2010). "L1 retrotransposition in neurons is modulated by MeCP2." Nature **468**(7322): 443-446.

Namihira, M., J. Kohyama, K. Semi, T. Sanosaka, B. Deneen, T. Taga and K. Nakashima (2009). "Committed neuronal precursors confer astrocytic potential on residual neural precursor cells." Dev Cell **16**(2): 245-255.

Nigumann, P., K. Redik, K. Matlik and M. Speek (2002). "Many human genes are transcribed from the antisense promoter of L1 retrotransposon." Genomics **79**(5): 628-634.

Nikitina, T., X. Shi, R. P. Ghosh, R. A. Horowitz-Scherer, J. C. Hansen and C. L. Woodcock (2007). "Multiple modes of interaction between the methylated DNA binding protein MeCP2 and chromatin." Mol Cell Biol **27**(3): 864-877.

Okabe, Y., T. Takahashi, C. Mitsumasu, K. Kosai, E. Tanaka and T. Matsuishi (2012). "Alterations of gene expression and glutamate clearance in astrocytes derived from an MeCP2-null mouse model of Rett syndrome." PLoS One **7**(4): e35354.

Ostertag, E. M. and H. H. Kazazian, Jr. (2001). "Twin priming: a proposed mechanism for the creation of inversions in L1 retrotransposition." Genome Res **11**(12): 2059-2065.

Pace, J. K., 2nd and C. Feschotte (2007). "The evolutionary history of human DNA transposons: evidence for intense activity in the primate lineage." Genome Res **17**(4): 422-432.

Pan, J. W., J. B. Lane, H. Hetherington and A. K. Percy (1999). "Rett syndrome: 1H spectroscopic imaging at 4.1 Tesla." J Child Neurol **14**(8): 524-528.

Piani, D., K. Frei, H. W. Pfister and A. Fontana (1993). "Glutamate uptake by astrocytes is inhibited by reactive oxygen intermediates but not by other macrophage-derived molecules including cytokines, leukotrienes or platelet-activating factor." J Neuroimmunol **48**(1): 99-104.

Robinson, S. R., A. Lee, G. M. Bishop, H. Czerwinska and R. Dringen (2015). "Inhibition of Astrocytic Glutamine Synthetase by Lead is Associated with a Slowed Clearance of Hydrogen Peroxide by the Glutathione System." Front Integr Neurosci **9**: 61.

Russo, F. B., B. C. Freitas, G. C. Pignatari, I. R. Fernandes, J. Sebat, A. R. Muotri and P. C. B. Beltrao-Braga (2018). "Modeling the Interplay Between Neurons and Astrocytes in Autism Using Human Induced Pluripotent Stem Cells." Biol Psychiatry **83**(7): 569-578.

Saleh, A., A. Macia and A. R. Muotri (2019). "Transposable Elements, Inflammation, and Neurological Disease." Front Neurol **10**: 894.

Sanalkumar, R., S. Vidyanand, C. Lalitha Indulekha and J. James (2010). "Neuronal vs. glial fate of embryonic stem cell-derived neural progenitors (ES-NPs) is determined by FGF2/EGF during proliferation." J Mol Neurosci **42**(1): 17-27.

Serio, A., B. Bilican, S. J. Barmada, D. M. Ando, C. Zhao, R. Siller, K. Burr, G. Haghi, D. Story, A. L. Nishimura, M. A. Carrasco, H. P. Phatnani, C. Shum, I. Wilmut, T. Maniatis, C. E. Shaw, S. Finkbeiner and S. Chandran (2013). "Astrocyte pathology and the absence of non-cell autonomy in an induced pluripotent stem cell model of TDP-43 proteinopathy." Proc Natl Acad Sci U S A **110**(12): 4697-4702.

Simon, M., M. Van Meter, J. Ablaeva, Z. Ke, R. S. Gonzalez, T. Taguchi, M. De Cecco, K. I. Leonova, V. Kogan, S. L. Helfand, N. Neretti, A. Roichman, H. Y. Cohen, M. V. Meer, V. N. Gladyshev, M. P. Antoch, A. V. Gudkov, J. M. Sedivy, A. Seluanov and V. Gorbunova (2019). "LINE1 Derepression in Aged Wild-Type and SIRT6-Deficient Mice Drives Inflammation." Cell Metab **29**(4): 871-885 e875.

Singer, T., M. J. McConnell, M. C. Marchetto, N. G. Coufal and F. H. Gage (2010). "LINE-1 retrotransposons: mediators of somatic variation in neuronal genomes?" Trends Neurosci **33**(8): 345-354.

Slotkin, R. K. and R. Martienssen (2007). "Transposable elements and the epigenetic regulation of the genome." Nat Rev Genet **8**(4): 272-285.

Smit, A. F. (1993). "Identification of a new, abundant superfamily of mammalian LTR-transposons." Nucleic Acids Res **21**(8): 1863-1872.

Song, C., Y. Feodorova, J. Guy, L. Peichl, K. L. Jost, H. Kimura, M. C. Cardoso, A. Bird, H. Leonhardt, B. Joffe and I. Solovei (2014). "DNA methylation reader MECP2: cell type- and differentiation stage-specific protein distribution." Epigenetics Chromatin **7**: 17.

Speek, M. (2001). "Antisense promoter of human L1 retrotransposon drives transcription of adjacent cellular genes." Mol Cell Biol **21**(6): 1973-1985.

Swergold, G. D. (1990). "Identification, characterization, and cell specificity of a human LINE-1 promoter." Mol Cell Biol **10**(12): 6718-6729.

Tharp, M. E., S. Malki and A. Bortvin (2020). "Maximizing the ovarian reserve in mice by evading LINE-1 genotoxicity." Nat Commun **11**(1): 330.

Thomas, C. A., L. Tejwani, C. A. Trujillo, P. D. Negraes, R. H. Herai, P. Mesci, A. Macia, Y. J. Crow and A. R. Muotri (2017). "Modeling of TREX1-Dependent Autoimmune Disease using Human Stem Cells Highlights L1 Accumulation as a Source of Neuroinflammation." Cell Stem Cell **21**(3): 319-331 e318.

Upton, K. R., D. J. Gerhardt, J. S. Jesuadian, S. R. Richardson, F. J. Sanchez-Luque, G. O. Bodea, A. D. Ewing, C. Salvador-Palomeque, M. S. van der Knaap, P. M. Brennan, A. Vanderver and G. J. Faulkner (2015). "Ubiquitous L1 mosaicism in hippocampal neurons." Cell **161**(2): 228-239.

van der Vaart, M., O. Svoboda, B. G. Weijts, R. Espin-Palazon, V. Sapp, T. Pietri, M. Bagnat, A. R. Muotri and D. Traver (2017). "Mecp2 regulates tnfa during zebrafish embryonic development and acute inflammation." Dis Model Mech **10**(12): 1439-1451.

Warkocki, Z., P. S. Krawczyk, D. Adamska, K. Bijata, J. L. Garcia-Perez and A. Dziembowski (2018). "Uridylation by TUT4/7 Restricts Retrotransposition of Human LINE-1s." Cell **174**(6): 1537-1548 e1529.

Williams, E. C., X. Zhong, A. Mohamed, R. Li, Y. Liu, Q. Dong, G. E. Ananiev, J. C. Mok, B. R. Lin, J. Lu, C. Chiao, R. Cherney, H. Li, S. C. Zhang and Q. Chang (2014). "Mutant astrocytes

differentiated from Rett syndrome patients-specific iPSCs have adverse effects on wild-type neurons." Hum Mol Genet **23**(11): 2968-2980.

Yang, N. and H. H. Kazazian, Jr. (2006). "L1 retrotransposition is suppressed by endogenously encoded small interfering RNAs in human cultured cells." Nat Struct Mol Biol **13**(9): 763-771.

Yasui, D. H., S. Peddada, M. C. Bieda, R. O. Vallero, A. Hogart, R. P. Nagarajan, K. N. Thatcher, P. J. Farnham and J. M. Lasalle (2007). "Integrated epigenomic analyses of neuronal MeCP2 reveal a role for long-range interaction with active genes." Proc Natl Acad Sci U S A **104**(49): 19416-19421.

Young, J. I., E. P. Hong, J. C. Castle, J. Crespo-Barreto, A. B. Bowman, M. F. Rose, D. Kang, R. Richman, J. M. Johnson, S. Berget and H. Y. Zoghbi (2005). "Regulation of RNA splicing by the methylation-dependent transcriptional repressor methyl-CpG binding protein 2." Proc Natl Acad Sci U S A **102**(49): 17551-17558.

Zhang, Z. N., B. C. Freitas, H. Qian, J. Lux, A. Acab, C. A. Trujillo, R. H. Herai, V. A. Nguyen Huu, J. H. Wen, S. Joshi-Barr, J. V. Karpiak, A. J. Engler, X. D. Fu, A. R. Muotri and A. Almutairi (2016). "Layered hydrogels accelerate iPSC-derived neuronal maturation and reveal migration defects caused by MeCP2 dysfunction." Proc Natl Acad Sci U S A **113**(12): 3185-3190.

Zhao, B., Q. Wu, A. Y. Ye, J. Guo, X. Zheng, X. Yang, L. Yan, Q. R. Liu, T. M. Hyde, L. Wei and A. Y. Huang (2019). "Somatic LINE-1 retrotransposition in cortical neurons and non-brain tissues of Rett patients and healthy individuals." PLoS Genet **15**(4): e1008043.